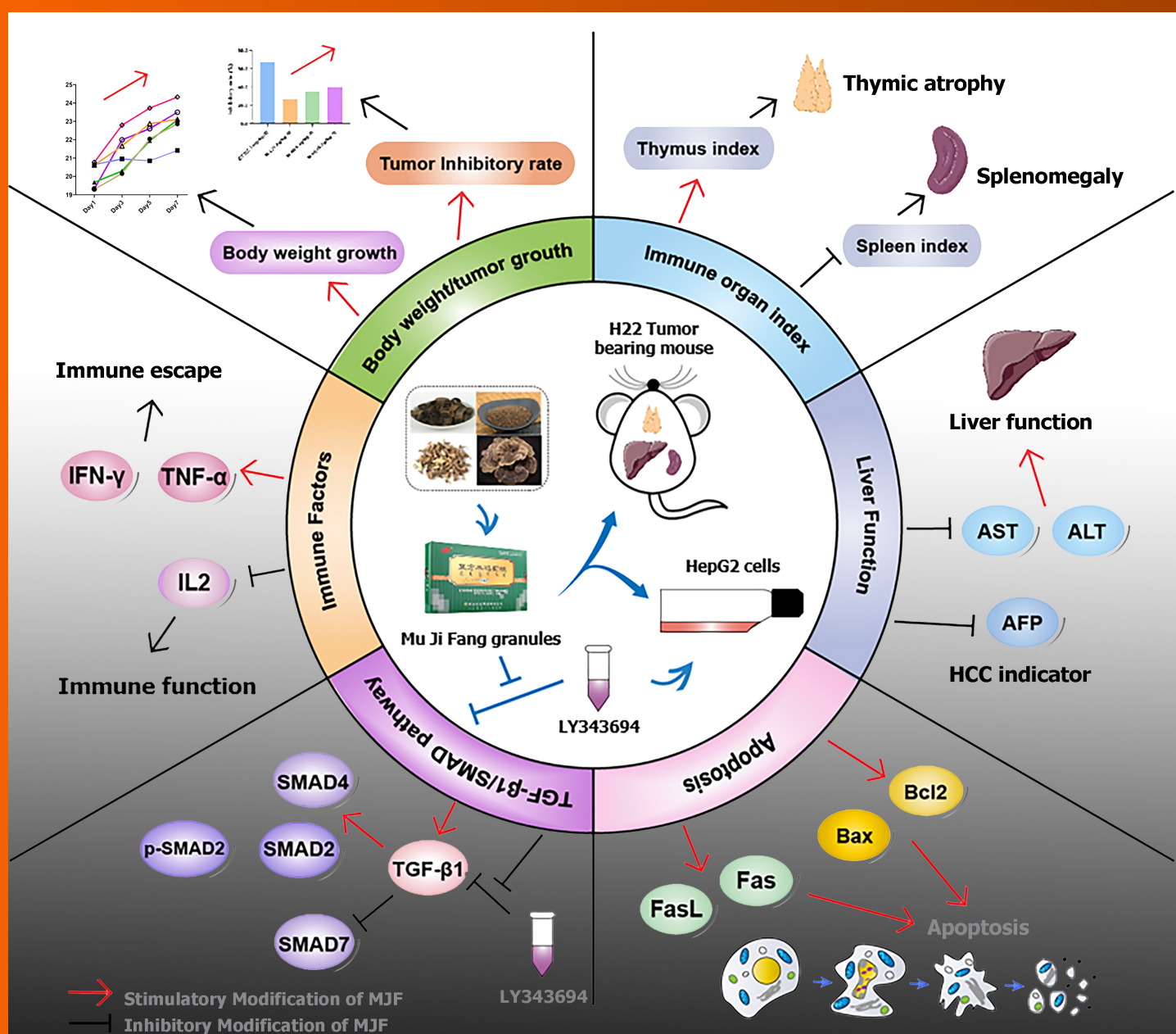


World Journal of Gastrointestinal Oncology

World J Gastrointest Oncol 2023 March 15; 15(3): 372-570



Overview of the possible anti-hepatocellular carcinoma effects of Mu Ji Fang Granules

FIELD OF VISION

- 372 Machine learning algorithm to construct cuproptosis- and immune-related prognosis prediction model for colon cancer
Huang YY, Bao TY, Huang XQ, Lan QW, Huang ZM, Chen YH, Hu ZD, Guo XG

REVIEW

- 389 Prevention of malignant digestive system tumors should focus on the control of chronic inflammation
Zhang YH, Chen XL, Wang YR, Hou YW, Zhang YD, Wang KJ
- 405 Immunotherapy for advanced or recurrent hepatocellular carcinoma
Luo YZ, Zhu H
- 425 Molecular methods for colorectal cancer screening: Progress with next-generation sequencing evolution
Abbes S, Baldi S, Sellami H, Amedei A, Keskes L

MINIREVIEWS

- 443 Genetic heterogeneity of colorectal cancer and the microbiome
Senchukova MA

ORIGINAL ARTICLE**Basic Study**

- 464 Xiaojianzhong decoction prevents gastric precancerous lesions in rats by inhibiting autophagy and glycolysis in gastric mucosal cells
Zhang JX, Bao SC, Chen J, Chen T, Wei HL, Zhou XY, Li JT, Yan SG
- 490 F-box and leucine-rich repeat 6 promotes gastric cancer progression *via* the promotion of epithelial-mesenchymal transition
Meng L, Hu YT, Xu AM
- 504 Possible mechanisms associated with immune escape and apoptosis on anti-hepatocellular carcinoma effect of Mu Ji Fang granules
Zhang YB, Bao YR, Wang S, Li TJ, Tai H, Leng JP, Yang XX, Wang BC, Meng XS

Retrospective Cohort Study

- 523 Risk of pancreatic cancer in individuals with celiac disease in the United States: A population-based matched cohort study
Krishnan A, Hadi YB, Shahih S, Mukherjee D, Patel RA, Patel R, Singh S, Thakkar S

Retrospective Study

- 533** Nomogram model predicting the overall survival for patients with primary gastric mucosa-associated lymphoid tissue lymphoma
Wang D, Shi XL, Xu W, Shi RH
- 546** Mitophagy-related gene signature predicts prognosis, immune infiltration and chemotherapy sensitivity in colorectal cancer
Weng JS, Huang JP, Yu W, Xiao J, Lin F, Lin KN, Zang WD, Ye Y, Lin JP

CASE REPORT

- 562** Carcinosarcoma of common bile duct: A case report
Yao Y, Xiang HG, Jin L, Xu M, Mao SY

ABOUT COVER

Zhang YB, Bao YR, Wang S, Li TJ, Tai H, Leng JP, Yang XX, Wang BC, Meng XS. Possible mechanisms associated with immune escape and apoptosis on anti-hepatocellular carcinoma effect of Mu Ji Fang granules. *World J Gastrointest Oncol* 2023; 15(3): 504-522 URL: <https://www.wjgnet.com/1948-5204/full/v15/i3/504.htm> DOI: <https://dx.doi.org/10.4251/wjgo.v15.i3.504>

AIMS AND SCOPE

The primary aim of *World Journal of Gastrointestinal Oncology* (*WJGO*, *World J Gastrointest Oncol*) is to provide scholars and readers from various fields of gastrointestinal oncology with a platform to publish high-quality basic and clinical research articles and communicate their research findings online.

WJGO mainly publishes articles reporting research results and findings obtained in the field of gastrointestinal oncology and covering a wide range of topics including liver cell adenoma, gastric neoplasms, appendiceal neoplasms, biliary tract neoplasms, hepatocellular carcinoma, pancreatic carcinoma, cecal neoplasms, colonic neoplasms, colorectal neoplasms, duodenal neoplasms, esophageal neoplasms, gallbladder neoplasms, etc.

INDEXING/ABSTRACTING

The *WJGO* is now abstracted and indexed in PubMed, PubMed Central, Science Citation Index Expanded (SCIE, also known as SciSearch®), Journal Citation Reports/Science Edition, Scopus, Reference Citation Analysis, China National Knowledge Infrastructure, China Science and Technology Journal Database, and Superstar Journals Database. The 2022 edition of Journal Citation Reports® cites the 2021 impact factor (IF) for *WJGO* as 3.404; IF without journal self cites: 3.357; 5-year IF: 3.250; Journal Citation Indicator: 0.53; Ranking: 162 among 245 journals in oncology; Quartile category: Q3; Ranking: 59 among 93 journals in gastroenterology and hepatology; and Quartile category: Q3. The *WJGO*'s CiteScore for 2021 is 3.6 and Scopus CiteScore rank 2021: Gastroenterology is 72/149; Oncology is 203/360.

RESPONSIBLE EDITORS FOR THIS ISSUE

Production Editor: Xiang-Di Zhang; Production Department Director: Xiang Li; Editorial Office Director: Jia-Ru Fan.

NAME OF JOURNAL

World Journal of Gastrointestinal Oncology

ISSN

ISSN 1948-5204 (online)

LAUNCH DATE

February 15, 2009

FREQUENCY

Monthly

EDITORS-IN-CHIEF

Monjur Ahmed, Florin Burada

EDITORIAL BOARD MEMBERS

<https://www.wjgnet.com/1948-5204/editorialboard.htm>

PUBLICATION DATE

March 15, 2023

COPYRIGHT

© 2023 Baishideng Publishing Group Inc

INSTRUCTIONS TO AUTHORS

<https://www.wjgnet.com/bpg/gerinfo/204>

GUIDELINES FOR ETHICS DOCUMENTS

<https://www.wjgnet.com/bpg/GerInfo/287>

GUIDELINES FOR NON-NATIVE SPEAKERS OF ENGLISH

<https://www.wjgnet.com/bpg/gerinfo/240>

PUBLICATION ETHICS

<https://www.wjgnet.com/bpg/GerInfo/288>

PUBLICATION MISCONDUCT

<https://www.wjgnet.com/bpg/gerinfo/208>

ARTICLE PROCESSING CHARGE

<https://www.wjgnet.com/bpg/gerinfo/242>

STEPS FOR SUBMITTING MANUSCRIPTS

<https://www.wjgnet.com/bpg/GerInfo/239>

ONLINE SUBMISSION

<https://www.f6publishing.com>



Basic Study

Xiaojianzhong decoction prevents gastric precancerous lesions in rats by inhibiting autophagy and glycolysis in gastric mucosal cells

Jia-Xiang Zhang, Sheng-Chuan Bao, Juan Chen, Ting Chen, Hai-Liang Wei, Xiao-Yan Zhou, Jing-Tao Li, Shu-Guang Yan

Specialty type: Gastroenterology and hepatology

Provenance and peer review:

Unsolicited article; Externally peer reviewed.

Peer-review model: Single blind

Peer-review report's scientific quality classification

Grade A (Excellent): 0
Grade B (Very good): B
Grade C (Good): C
Grade D (Fair): 0
Grade E (Poor): 0

P-Reviewer: Cabezuelo AS, Spain;
Liu YQ, United States

Received: August 16, 2022

Peer-review started: August 16, 2022

First decision: November 17, 2022

Revised: December 1, 2022

Accepted: January 16, 2023

Article in press: January 16, 2023

Published online: March 15, 2023



Jia-Xiang Zhang, Sheng-Chuan Bao, Juan Chen, Ting Chen, Shu-Guang Yan, College of Basic Medicine, Shaanxi University of Chinese Medicine, Xianyang 712046, Shaanxi Province, China

Jia-Xiang Zhang, Sheng-Chuan Bao, Juan Chen, Ting Chen, Hai-Liang Wei, Xiao-Yan Zhou, Shu-Guang Yan, Key Laboratory of Gastrointestinal Diseases and Prescriptions in Shaanxi Province, Shaanxi University of Chinese Medicine, Xianyang 712046, Shaanxi Province, China

Hai-Liang Wei, Department of General Surgery, The Affiliated Hospital of Shaanxi University of Chinese Medicine, Xianyang 712000, Shaanxi Province, China

Xiao-Yan Zhou, Department of Gastroenterology, The Affiliated Hospital of Shaanxi University of Chinese Medicine, Xianyang 712000, Shaanxi Province, China

Jing-Tao Li, Departments of Infectious Disease, The Affiliated Hospital of Shaanxi University of Chinese Medicine, Xianyang 712000, Shaanxi Province, China

Corresponding author: Shu-Guang Yan, PhD, Professor, College of Basic Medicine, Shaanxi University of Traditional Chinese Medicine, Century Avenue, Qindu District, Xianyang 712046, Shaanxi Province, China. ygs2002.student@sina.com

Abstract

BACKGROUND

Gastric precancerous lesions (GPL) precede the development of gastric cancer (GC). They are characterized by gastric mucosal intestinal metaplasia and dysplasia caused by various factors such as inflammation, bacterial infection, and injury. Abnormalities in autophagy and glycolysis affect GPL progression, and their effective regulation can aid in GPL treatment and GC prevention. Xiaojianzhong decoction (XJZ) is a classic compound for the treatment of digestive system diseases in ancient China which can inhibit the progression of GPL. However, its specific mechanism of action is still unclear.

AIM

To investigate the therapeutic effects of XJZ decoction on a rat GPL model and the mechanisms underlying its effects on autophagy and glycolysis regulation in GPLs.

METHODS

Wistar rats were randomly divided into six groups of five rats each and all groups except the control group were subjected to GPL model construction for 18 wk. The rats' body weight was monitored every 2 wk starting from the beginning of modeling. Gastric histopathology was examined using hematoxylin-eosin staining and Alcian blue-periodic acid-Schiff staining. Autophagy was observed using transmission electron microscopy. The expressions of autophagy, hypoxia, and glycolysis related proteins in gastric mucosa were detected using immunohistochemistry and immunofluorescence. The expressions of the following proteins in gastric tissues: B cell lymphoma/Leukemia-2 and adenovirus E1B19000 interacting protein 3 (Bnip-3), microtubule associated protein 1 light chain 3 (LC-3), moesin-like BCL2-interacting protein 1 (Beclin-1), phosphatidylinositol 3-kinase (PI3K), protein kinase B (AKT), mammalian target of rapamycin (mTOR), p53, AMP-activated protein kinase (AMPK), and Unc-51 like kinase 1 (ULK1) were detected using western blot. The relative expressions of autophagy, hypoxia, and glycolysis related mRNA in gastric tissues was detected using reverse transcription-polymerase chain reaction.

RESULTS

Treatment with XJZ increased the rats' body weight and improved GPL-related histopathological manifestations. It also decreased autophagosome and autolysosome formation in gastric tissues and reduced Bnip-3, Beclin-1, and LC-3II expressions, resulting in inhibition of autophagy. Moreover, XJZ down-regulated glycolysis-related monocarboxylate transporter (MCT1), MCT4, and CD147 expressions. XJZ prevented the increase of autophagy level by decreasing gastric mucosal hypoxia, activating the PI3K/AKT/mTOR pathway, inhibiting the p53/AMPK pathway activation and ULK1 Ser-317 and Ser-555 phosphorylation. In addition, XJZ improved abnormal gastric mucosal glucose metabolism by ameliorating gastric mucosal hypoxia and inhibiting ULK1 expression.

CONCLUSION

This study demonstrates that XJZ may inhibit autophagy and glycolysis in GPL gastric mucosal cells by improving gastric mucosal hypoxia and regulating PI3K/AKT/mTOR and p53/AMPK/ULK1 signaling pathways, providing a feasible strategy for the GPL treatment.

Key Words: Xiaojianzhong decoction; Gastric precancerous lesions; Autophagy; Glycolysis; Gastric mucosal cells; Herb

©The Author(s) 2023. Published by Baishideng Publishing Group Inc. All rights reserved.

Core Tip: Xiaojianzhong Decoction is a classic compound for the treatment of digestive system diseases in ancient China, and it also shows good curative effect in the treatment of gastric precancerous lesions (GPL). Many studies have shown that the levels of autophagy and glycolysis influence the progression of GPL. Our study found that Xiaojianzhong Decoction can improve the pathological manifestations of gastric mucosa in GPL rats, and inhibits the expression of autophagy, glycolysis-related proteins and mRNA. Xiaojianzhong decoction (XJZ) prevented the increase of autophagy levels by decreasing gastric mucosal hypoxia, activating the phosphatidylinositol 3-kinase/protein kinase B/mammalian target of rapamycin pathway, inhibiting the p53/AMP-activated protein kinase pathway activation and Unc-51 Like kinase 1 (ULK1) Ser-317 and Ser-555 phosphorylation. In addition, XJZ improved abnormal gastric mucosal glucose metabolism by ameliorating gastric mucosal hypoxia and inhibiting ULK1 expression.

Citation: Zhang JX, Bao SC, Chen J, Chen T, Wei HL, Zhou XY, Li JT, Yan SG. Xiaojianzhong decoction prevents gastric precancerous lesions in rats by inhibiting autophagy and glycolysis in gastric mucosal cells. *World J Gastrointest Oncol* 2023; 15(3): 464-489

URL: <https://www.wjgnet.com/1948-5204/full/v15/i3/464.htm>

DOI: <https://dx.doi.org/10.4251/wjgo.v15.i3.464>

INTRODUCTION

Gastric precancerous lesions (GPLs) are histopathological changes of the gastric mucosa that are prone to cancer, mainly including intestinal metaplasia (IM) and dysplasia (Dys), accompanied by local mucosal inflammation and atrophy[1]. As an early pathological process before the occurrence of gastric cancer (GC), GPL is reversible, and preventing the progression of GPL can reduce the morbidity and

mortality of GC, so it is significant to carry out early prevention and treatment in the GPL stage. Epidemiological surveys show that the incidence of GPL in patients undergoing endoscopy in East Asia is as high as 23.2%; among them, 32.0% have IM and 10.6% have Dys, and the incidence of GC in these patients is 23.8% and 7.3%, respectively. Thus, the prevention and treatment of GPLs are crucial and urgent[2].

GPL occurs in the epithelial cells and glands of the gastric mucosa. The continuous action of multiple factors such as *Helicobacter pylori* infection and inflammatory injury causes gastric mucosal cells to atrophy or decrease in number, and the abnormal repair of the gastric mucosa causes the replacement of lamina propria glands by goblet cells and the gradual development of IM and Dys. Autophagy is a process in which cells autonomously generate autophagosomes to phagocytose intracellular functionally damaged or senescent cell structures and then combine with lysosomes for digestion, energy production, and reuse by the body. As an important factor affecting the fate of IM and Dys cells, autophagy is present throughout the course of GPL[3]. An appropriate level of autophagy maintains intracellular homeostasis and avoids the accumulation of gene damage or even canceration. The complex local microenvironment comprising hypoxia, ischemia, and dysregulation of the signaling molecule activation in GPLs leads to increased autophagy. This increase in autophagy not only helps the GPL dysplastic cells to repair damaged organelles, maintain the stability of the internal environment, and ensure survival but also increases the damage and death of normal gastric mucosal cells[4,5]. Thus, inhibition of high levels of autophagy in gastric mucosal cells may be effective in preventing GPL progression. However, there is currently a lack of drugs that can inhibit autophagy in gastric mucosal cells and effectively treat GPL. Moreover, the complex local microenvironment of the GPL gastric mucosa is a favorable condition for activating glycolysis. Many studies have shown that cells in the GPL stage have high levels of glycolysis. Glycolysis accelerates adenosine triphosphate (ATP) production and promotes the proliferation of dysplastic cells in the gastric mucosa and the accumulation of lactate. The end product of this process promotes the formation of an acidic microenvironment in the gastric mucosa which facilitates tumor occurrence and development[6,7]. In summary, the activation of glycolysis and high levels of autophagy may together contribute to GPL deterioration.

Accumulating evidence indicates that natural medicines and their formulations play a unique role in the treatment of digestive diseases. In recent years, the discovery of natural medicines has occupied an important position in the field of new drug development. It is very promising to find safer and more effective natural medicines and foods against GPL. Xiaojianzhong decoction (XJZ), the formula of which comes from the ancient Chinese medical practitioner Zhang Zhongjing's *Treatise on Febrile and Miscellaneous Diseases*, is a classic traditional Chinese medicine compound for the treatment of gastrointestinal diseases and contains six edible herbal medicines: Maltose, cassia twig, paeonia lactiflora, ginger, licorice, and jujube. Studies have found that the main components of these drugs have certain therapeutic effects on the diseased gastric mucosa. For example, cinnamaldehyde and 6-shogaol can inhibit autophagy of gastric mucosal cells, inhibit Hp reproduction, and have anti-inflammatory and analgesic effects[8,9]; paeoniflorin can regulate immune function, act as antioxidants, and inhibits glycolysis[10].

Therefore, in this study, we investigated the therapeutic effects of XJZ on GPL and its underlying mechanisms by constructing a rat GPL model with N-methyl-N'-nitro-N-nitrosoguanidine (MNNG), with the aim of assessing the potential of XJZ as a therapeutic drug for GPL.

MATERIALS AND METHODS

Chemicals and reagents

The ingredients-maltose, cassia twig, paeonia lactiflora, ginger, licorice, and jujube-of XJZ were purchased from Xingshengde Pharmaceutical Co., Ltd. (Xi'an, China). MNNG and Tretinoin were purchased from Solarbio Technology Co., Ltd. (Beijing, China). Superoxide dismutase (SOD) and malondialdehyde (MDA) biochemical detection kits were purchased from Nanjing Jiancheng Bioengineering Institute (Nanjing, Jiangsu Province, China). Alanine aminotransferase (ALT) and creatinine (Cr) biochemical detection kits were purchased from Changchun Huili Biotechnology Co., Ltd. (Changchun, Jilin Province, China). Caudal-type homeobox protein 2 (CDX-2), Ki-67, p62, Sirtuin 6 (SIRT6), microtubule associated protein 1 Light chain 3 (LC-3), and moesin-like BCL2-interacting protein 1 (Beclin-1) antibodies were purchased from Proteintech Group, Inc (Wuhan, Hubei Province, China). Phosphatidylinositol 3-kinase (PI3K)/p-PI3K, protein kinase B (AKT)/p-AKT, mammalian target of rapamycin (mTOR)/p-mTOR, Unc-51 Like kinase 1 (ULK1)/p-ULK1 Ser-317/p-ULK1 Ser-555, p53/p-p53, and AMP-activated protein kinase (AMPK)/p-AMPK antibodies were purchased from ABCAM (United States). Hypoxia-inducible factor-1 α (HIF-1 α), B cell lymphoma/leukemia-2 and adenovirus E1B19000 interacting protein 3 (Bnip-3), and CD147 antibodies were purchased from Wuhan Boster Biological Technology Co., Ltd. (Wuhan, Hubei Province, China). Trizol and Western blot chemiluminescence reagents were purchased from Ambion Thermo Fisher Scientific CN (Shanghai, China).

Animal model construction and sampling

The male Wistar rats used in this study, which were provided by Beijing Spelford Laboratory Animal Co., Ltd, were housed in specific pathogen free-class animal rooms. All the animal experiments were approved by the Experimental Animal Ethics Committee of Shaanxi University of Chinese Medicine. Every effort was made to reduce the number of animals used and alleviate their suffering. As presented in **Figure 1A**, routinely fed with water and food. They were acclimatized for 1 wk and then divided into six groups (five rats per group) according to random number method: Control, model (MNNG, 180 mg/L, free to be drunk in the dark; hot ranitidine-salt solution, 2.25 g/L, 40 °C; and 20% ethanol, 2.50 mL/d), XJZ-L (low dose of XJZ, 1.875 g/kg; MNNG, 180 mg/L; hot ranitidine-salt solution, 2.25 g/L, 40 °C; and 20% ethanol 2.50 mL/d), XJZ-M (middle dose of XJZ, 3.75 g/kg; MNNG, 180 mg/L; hot ranitidine-salt solution, 2.25 g/L, 40 °C; 20% ethanol 2.50 mL/d), XJZ-H (high dose of XJZ, 7.50 g/kg; MNNG, 180 mg/L, hot ranitidine-salt solution, 2.25 g/L, 40 °C; and 20% ethanol 2.50 mL/d), and tretinoin (tretinoin, 0.04 g/kg; MNNG, 180 mg/L; hot ranitidine-salt solution, 2.25 g/L, 40 °C; and 20% ethanol, 2.50 mL/d). The model was constructed by the MNNG compound modeling method (MNNG was free to be drunk in the dark, and hot ranitidine-salt solution and 20% ethanol were alternately gavaged) combined with "starvation-satiation alternation". After 18 wk, the control and model groups were gavaged with saline, and the remaining four groups were gavaged with the corresponding concentrations of drugs. After 4 wk of intervention, pentobarbital anesthesia was administered. Blood was collected from the abdominal aorta and centrifuged; next, the serum was extracted and frozen in an ultra-low temperature refrigerator. The whole stomach was cut along the greater curvature, and the tissue at the junction between the gastric body and the gastric antrum was taken. Two pieces of flat gastric tissue were cut. One was fixed in 2.5% glutaraldehyde, and stored at 4 °C for transmission electron microscopy; the other was fixed in 4.0% paraformaldehyde for immunofluorescence, immunohistochemistry, and pathological staining. The remaining tissues were placed in cryovials and frozen with liquid nitrogen for protein and mRNA detection.

High-performance liquid chromatography

First, we collected 9 g of paeonia lactiflora, 9 g of cassia twig, 6 g of licorice, 9 g of ginger, six jujubes (24 g), and 30 g of maltose and added 11.5 times of water. The mixture was soaked for 30 min, decocted for 1.5 h, and then filtered. Next, eight times of water was added to the filter residue, and the mixture was decocted for 1 h and filtered. The filtrates were combined. Maltose (30 g) was added to melt, and the mixture was concentrated to 1.05 mg/mL of raw drug and then centrifuged. Subsequently, 1 mL of the centrifuge was taken, and methanol was added until the volume was 10 mL. After coarse filtration, the filtrate was passed through a 0.22 µm microporous membrane to obtain the injection solution. Chromatographic column: Acuity-I-Class UPLC-BEH C18 column (2.1 mm × 100.0 mm, 1.7 µm); mobile phase: Acetonitrile (A)-0.1% phosphoric acid water; volume flow rate: 0.2 mL/min; column temperature: 30 °C; and injection volume: 2 µL.

Body weight monitoring

Each rat was weighed every 16 d. At each measurement, the rats were weighed several times until stable weight values were obtained continuously to ensure accurate monitoring results.

Histopathological analysis

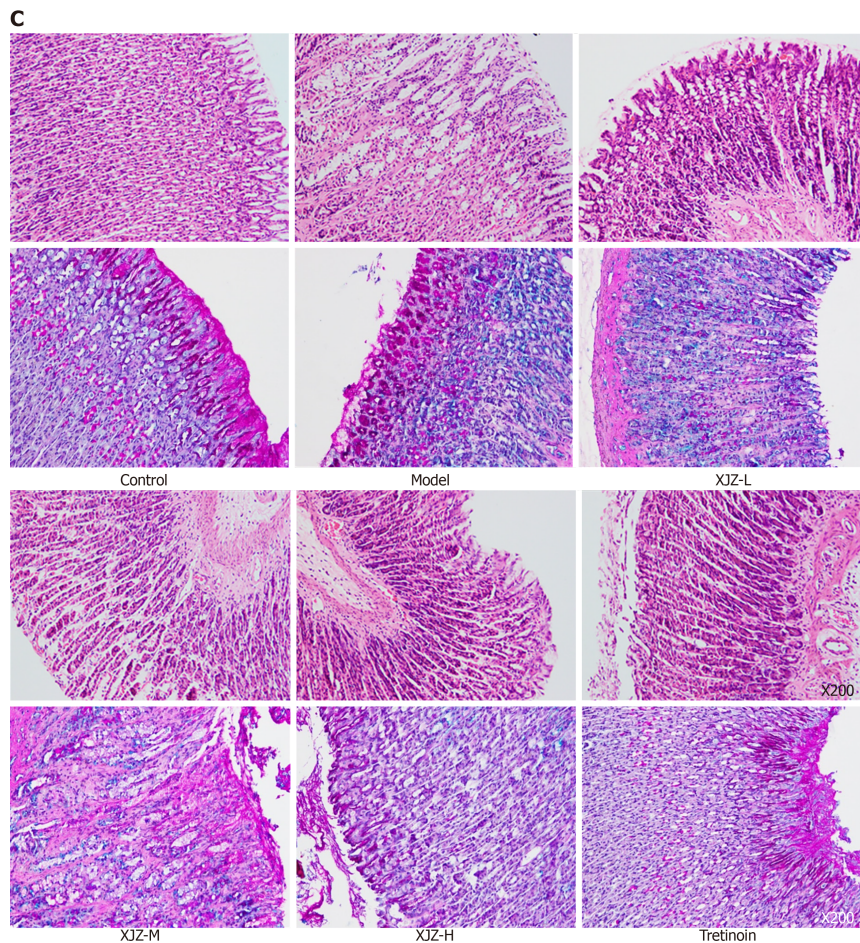
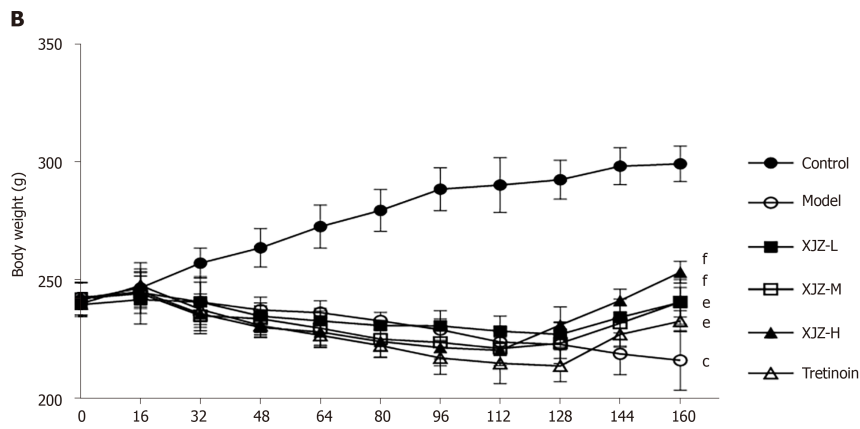
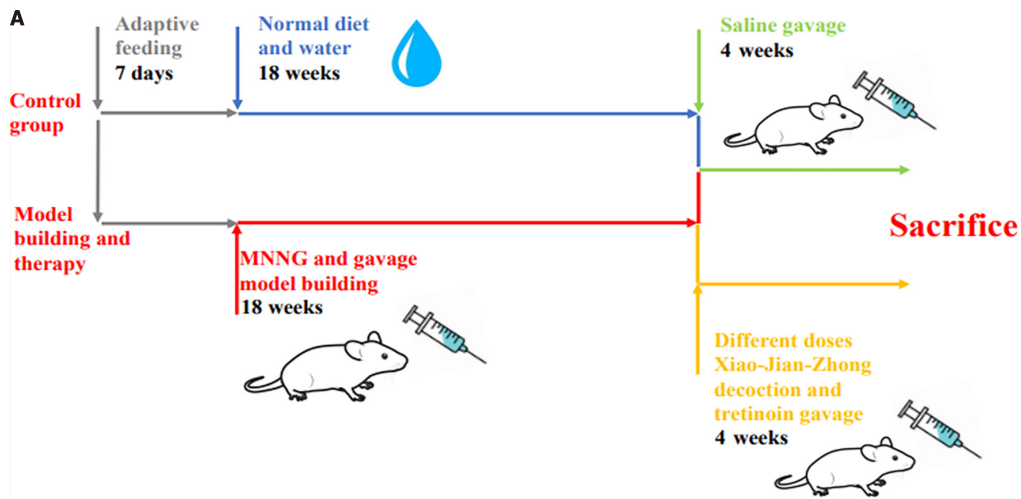
The fixed gastric tissues were dehydrated, paraffin-embedded, and sectioned into 2-µm-thick slices, deparaffinized, and rehydrated using an ethanol gradient. Gastric tissues were stained using hematoxylin-eosin (H&E) and alcian blue-periodic acid-Schiff (AB-PAS) staining. The images were collected using light microscopy.

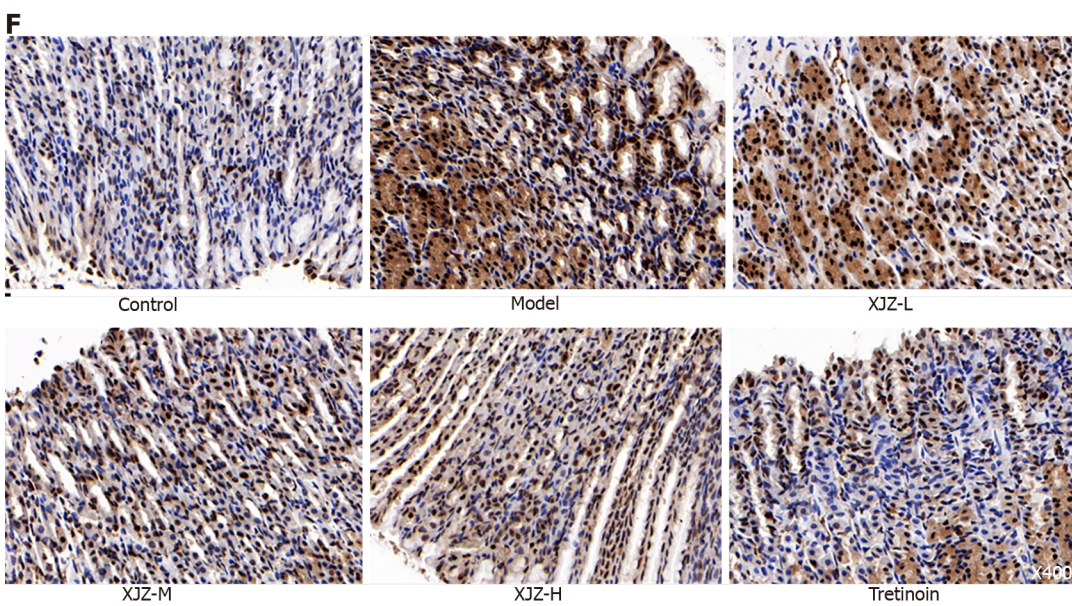
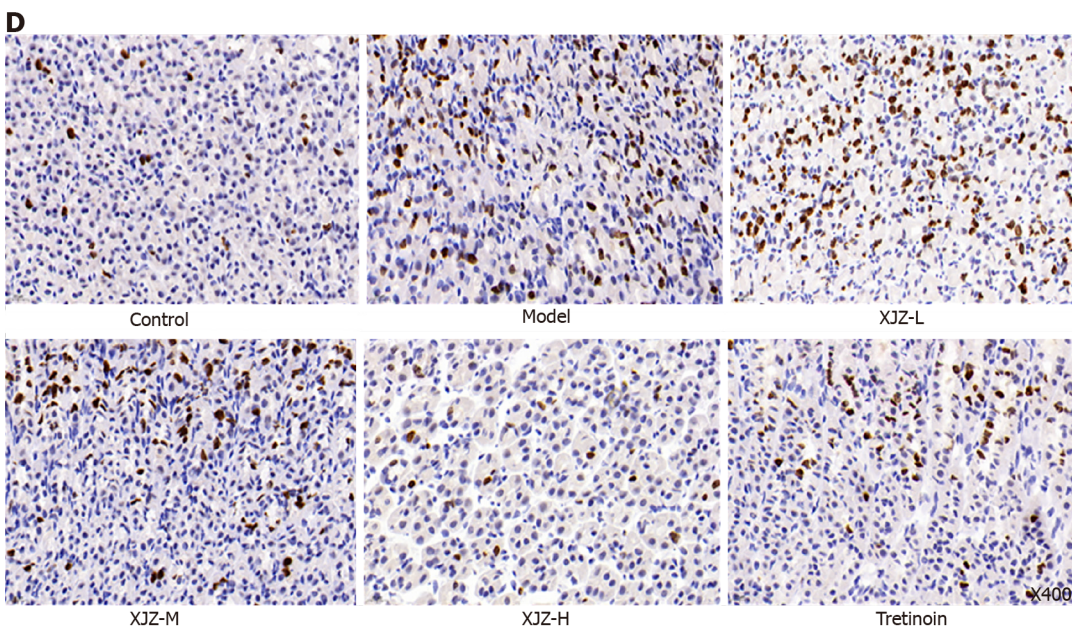
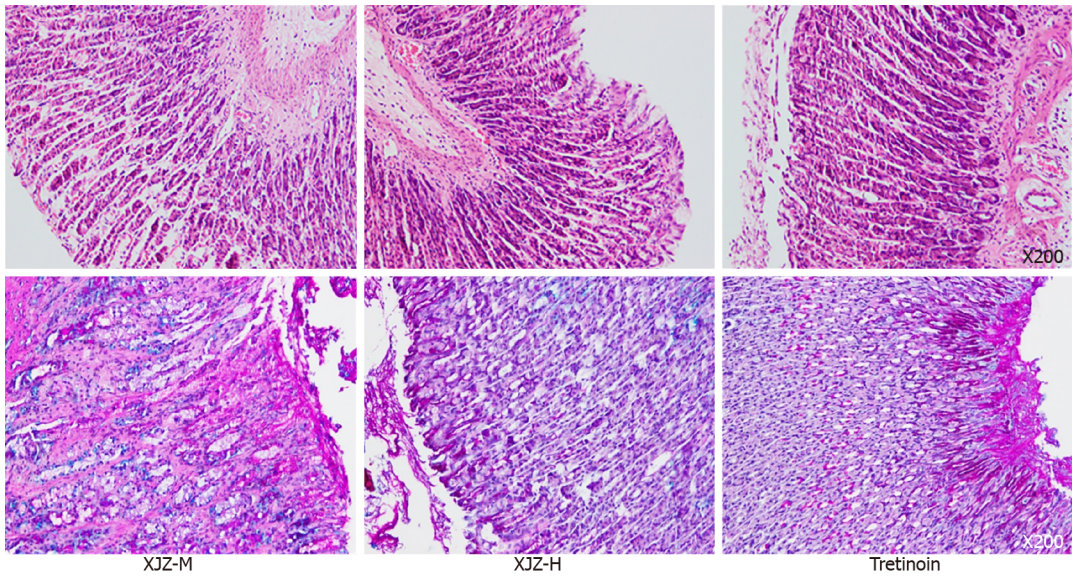
Serum biochemical test

Serum ALT, Cr, MDA, and SOD were detected using a Rayto automatic biochemical analyzer and a FlexStation3 multimode microplate reader (Molecular Devices) according to the manufacturers' instructions.

Transmission electron microscopy

After the gastric tissues were fixed in glutaraldehyde for 3-4 h, the cells were collected by scraping, centrifuged at 1000 rpm to settle the cells, and placed again in 2.5% glutaraldehyde for 4 h at 4 °C. The cells were rinsed three times for 15 min each in 0.1 M phosphate buffer. Next, 1% osmic acid-phosphate buffer was used to fix the cells at room temperature (20 °C) for 2 h and the ethanol gradient was used to dehydrate the cells for 15 min/time. The cells were infiltrated overnight with a mixture of acetone and 812 embedding medium (1:1), followed by pure 812 embedding medium overnight. After embedding and sectioning, the uranium-lead double staining solution was used to stain the cells for 15 min, and the sections were dried at room temperature overnight. Images were observed and acquired under an electron microscope.





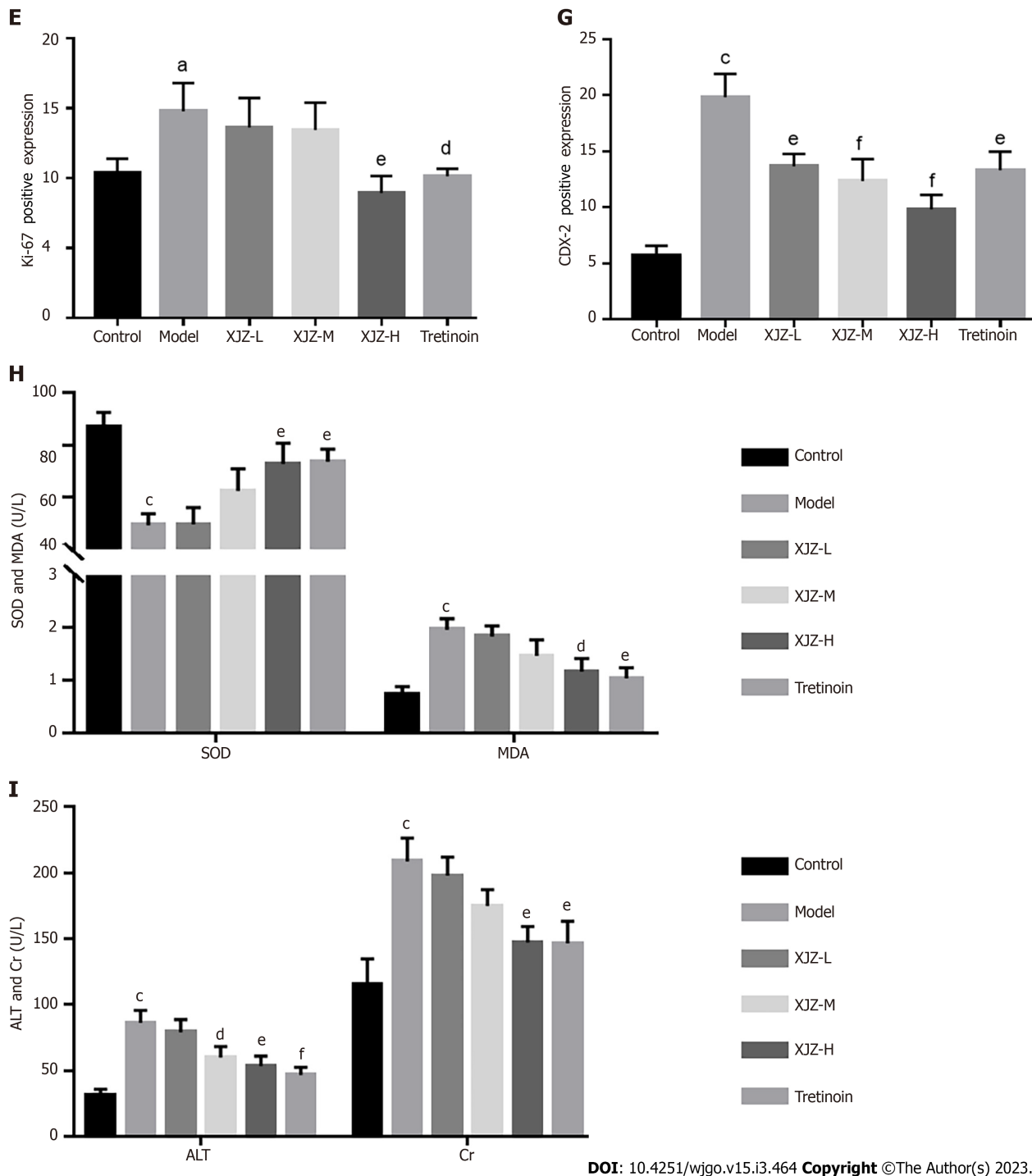


Figure 1 Effects of Xiaojianzhong decoction on body weight, gastric mucosal pathological conditions and liver kidney toxicity in N-methyl-N'-nitro-N-nitrosoguanidine-induced gastric precancerous lesions rats. A: Schematic diagram of model construction and treatment; B: Schematic diagram of weight change in rats; C: Representative images of hematoxylin-eosin and alcian blue-periodic acid-Schiff staining of gastric tissues; D-G: Ki-67 and caudal-type homeobox protein 2 (CDX-2) expression was determined using immunohistochemistry (n = 5); Ki-67 and CDX-2 positive score was determined using Image J; H: Superoxide dismutase and malondialdehyde levels in serum (n = 3); I: Alanine aminotransferase and creatinine levels in serum (n = 3). Data are expressed as mean ± SD. ^aP < 0.05, ^bP < 0.01, ^cP < 0.001 vs control group; ^dP < 0.05, ^eP < 0.01, ^fP < 0.001 vs model group. XJZ-L: Low dose of Xiaojianzhong decoction; XJZ-M: Middle dose of Xiaojianzhong decoction; XJZ-H: High dose of Xiaojianzhong decoction; SOD: Superoxide dismutase; MDA: Malondialdehyde; ALT: Alanine aminotransferase; Cr: Creatinine.

Immunohistochemical analysis

Paraffin sections (3 μm thick) were deparaffinized and then rehydrated with an ethanol gradient. The sections were incubated with 3% H₂O₂ to remove endogenous peroxidase and then incubated with Ki-67, CDX-2, p62, and SIRT6 antibodies (1:100) overnight at 4 °C, followed by incubation with HRP-conjugated secondary antibodies at 37 °C for 30 min. The sections were then stained with hematoxylin and observed under sealed conditions. Images were collected.

Immunofluorescence analysis

Gastric tissue sections were deparaffinized and subjected to antigen retrieval and serum blocking. The sections were then incubated with HIF-1 α , Bnip-3, Beclin-1, and CD147 antibodies (1:100) overnight at 4 °C, rinsed with PBST, incubated with diluted fluorescent secondary antibodies for 1 h at 37 °C, and rinsed with PBST. After that, the sections were incubated with DAPI in the dark to stain the nuclei, and the excess DAPI was washed off by PBST. The sections were sealed with a mounting solution containing an anti-fluorescence quencher, and images were collected using a laser confocal fluorescence microscope.

Western blot analysis

Gastric tissue samples were placed in a 2-mL EP tube and lysed and homogenized with 200 μ L of lysis buffer. After being fully lysed on ice, the lysate was transferred to a centrifuge tube and centrifuged at 4 °C and 12000 rpm for 5 min, and the supernatant was separated into centrifuge tubes and placed at -20 °C. The protein samples and standard proteins diluted with PBS were added to 96-well plates and incubated for 15 min at 37 °C in the dark. The protein supernatant and buffer were incubated in a boiling water bath. The prepared protein samples and MAKER were added to the loading wells for electrophoresis blocking and membrane transfer. Next, 5% skim milk powder was added and blocked the membrane at room temperature on a shaker for 2 h. The PVDF membrane was then mixed with antibodies against HIF-1 α (1:4000), Bnip-3 (1:1000), LC-3 (1:4000), Beclin-1 (1:1000), p-PI3K (1:1000), and PI3K (1:1000), p-AKT (1:3000), AKT (1:2000), p-mTOR (1:5000), mTOR (1:10000), p-p53 (1:1000), p53 (1:1000), p-AMPK (1:1000), AMPK (1:2000), p-ULK1 ser317 (1:1000), p-ULK1 ser555 (1:1000), ULK1 (1:1000), β -actin (1:1000), and Lamin B (1:1000) for overnight incubation at 4 °C. The PVDF membranes were washed well with TBST five times and incubated with secondary antibodies for 2 h. Protein bands were visualized using an ELC reagent followed by exposure on X-ray film ([Supplementary material](#)).

Reverse transcription-polymerase chain reaction analysis

The gastric tissue was added with 1 mL of Trizol reagent, ground into a pulp with a homogenizer, and transferred to an RNase-free 1.5-mL EP tube for lysis for 10 min. Next, 200 μ L of chloroform was added and mixed well; the mixture was placed at room temperature for 5 min and centrifuged at 4 °C and 12000 rpm for 8 min. The upper aqueous phase was transferred to a new 1.5 mL EP tube, and 400 μ L of isopropanol was added. The mixture was mixed well, placed at room temperature for 10 min, and centrifuged at 4 °C and 12000 rpm for 10 min. The supernatant was discarded and 1 mL of RNase-free 75% ethanol was added. The mixture was vortexed and mixed well, followed by centrifugation at 10000 rpm for 5 min at 4 °C. The supernatant was discarded, the RNA precipitate was dried for 5-10 min, and the precipitate was dissolved in 20 μ L of DEPC water. Then, 2 μ L of dissolved RNA was taken, and the purity and concentration of RNA were calculated using a microspectrophotometer (see [Table 1](#) for primer sequences).

Statistical analysis

All quantitative data are presented as mean \pm SD. Statistical analysis was performed using GraphPad Prism version 7 (GraphPad Software Inc., San Diego, CA, United States). Comparisons between the groups were performed using a one-way analysis of variance, whereas multiple comparisons were performed using LSD. Statistical significance was set at $P < 0.05$, $P < 0.01$, or $P < 0.001$.

RESULTS

Chemical profiling of the constituents in XJZ

We analyzed the main components of XJZ using UPLC-Q-Orbitrap HRMS and successfully identified the main components of XJZ, which is recommended by the Chinese Pharmacopoeia 2020. The results showed that XJZ samples contained abundant chromatographic peaks ([Figure 2A](#)), indicating the presence of a large number of natural constituents, including albiflorin, paeoniflorin, liquiritin, cinnamaldehyde, and 6-gingerol ([Figure 2B-F](#)).

XJZ prevents MNNG-induced GPL progression in rats

MNNG is typically used to construct a GPL animal model because it has the advantages of high stability and easy administration[11]. In this experiment, GPL was successfully induced in rats by a compound modeling method of drinking MNNG freely in the dark + 20% ethanol/hot saline-ranitidine by alternating gavage + alternating "satiating-starvation" ([Figure 1A](#)). After 4 wk of treatment, we observed that XJZ increased the body weight of rats in a time- and dose-dependent manner ([Figure 1B](#)), ameliorated the morphological abnormalities of gastric mucosa in GPL rats in a dose-dependent manner, promoted the restoration of the integrity and regularity of the gastric mucosal gland structures and reduced the secretion of IM acidic mucus in the gastric mucosa ([Figure 1C](#)). In addition to the disorder of glandular structure and the secretion of acidic mucus, the gastric mucosa of GPL also shows

Table 1 Primer pair sequences

Gene	Primer	Sequence, 5'-3'	PCR products
B-actin	Forward	CACGATGGAGGGCCGGACTCATC	240 bp
	Reverse	TAAAGACCTCTATGCCAACACAGT	
Rat PI3K	Forward	GCAACAAGTCCTCTGCCCCAA	222 bp
	Reverse	ACGTAATAGAGGAGCTGGGC	
Rat AKT	Forward	GCTCTTCTCCACCTGTCTCG	186 bp
	Reverse	CACAGCCCCAAGTCCGTTA	
Rat mTOR	Forward	GAGATACGCCGTCATTCCT	199 bp
	Reverse	ATGCTCAAACACCTCCACC	
Rat HIF-1 α	Forward	GCGGCGAGAACGAGAAGAAAAATAG	129 bp
	Reverse	GAAGTGGCAACTGATGAGCAAG	
Rat MCT1	Forward	TGTATGCCGGAGGTCCTATC	177 bp
	Reverse	AGTTGAAAGCAAGCCCAAGA	
Rat MCT4	Forward	ACGGCAGGTTTCATAACAGG	162 bp
	Reverse	GCCATACGAGATCCCAAAGA	
Rat Bnip-3	Forward	GGTCAAGTCGGCCAGAAAAT	207 bp
	Reverse	TGTCTCAGACGCCTTCCAATG	
Rat LC3	Forward	AAAATGGGGCACGGATGAAG	155 bp
	Reverse	GCAGGTCTTCAAAAATGCCCA	
Rat CDX-2	Forward	TCTCCGAGAGGCAGGTTAAA	186 bp
	Reverse	GCAAGGAGGTCACAGGACTC	
Homo ULK1	Forward	TTATCATGTCCCAGCACTACGAT	242 bp
	Reverse	AAATTCATCAAAGTCCATGCCGT	
Rat CD147	Forward	GGCACCATCGTAACCTCTGT	211 bp
	Reverse	CAGGCTCAGGAAGGAAGATG	
Rat Beclin-1	Forward	GAGGTACCGACTTGTTCCT	225 bp
	Reverse	CCTTTCTCCACGTCCATCCT	

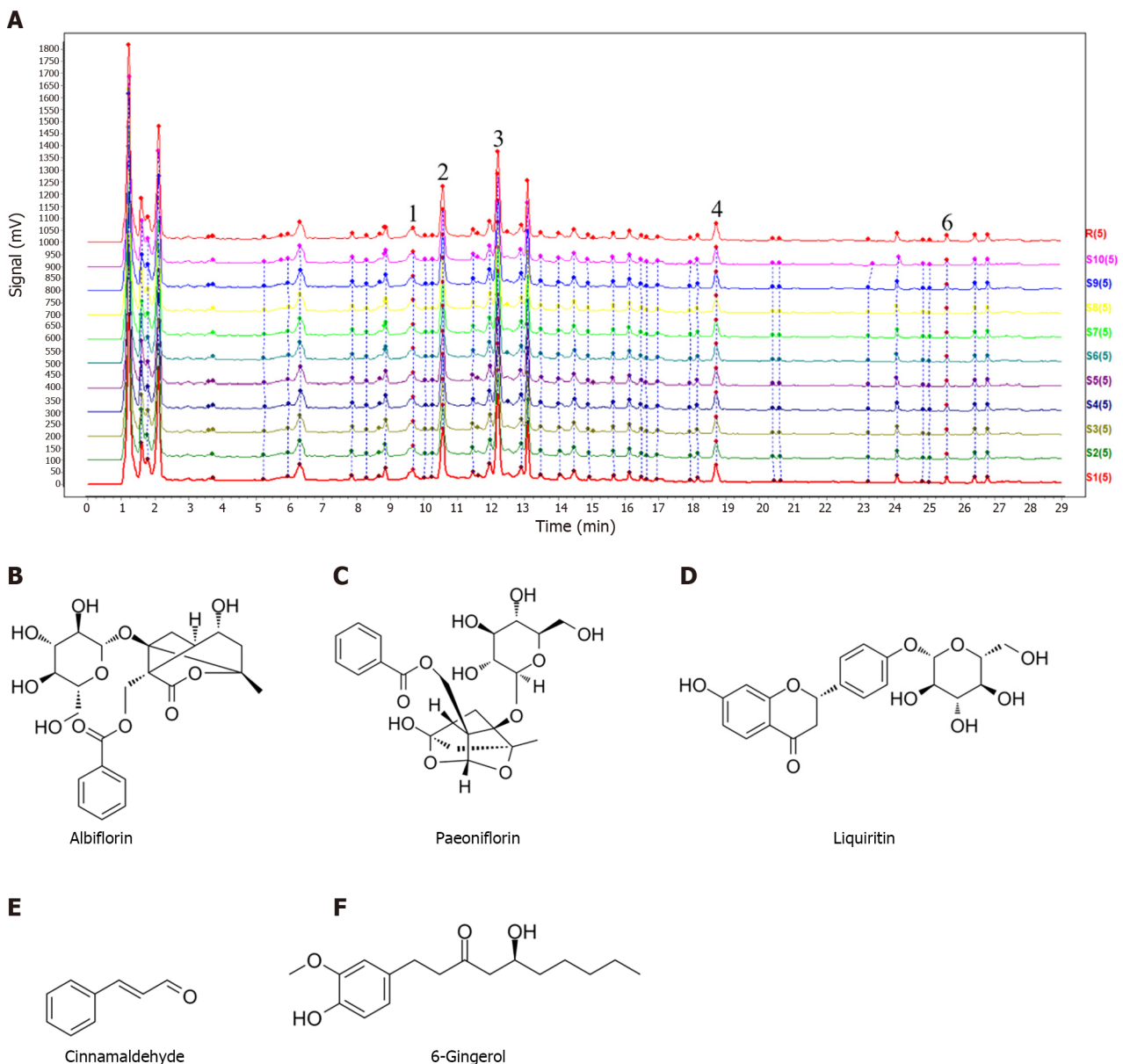
AKT: Protein kinase B; Beclin-1: Moesin-like BCL2-interacting protein 1; Bnip-3: B cell lymphoma/Leukemia-2 and adenovirus E1B19000 interacting protein 3; HIF-1 α : Hypoxia-inducible factor-1 α ; LC-3: Microtubule associated protein 1 light chain 3; PCR: Polymerase chain reaction; PI3K: Phosphatidylinositol 3-kinase; MCT: Monocarboxylate transporter; mTOR: Mammalian target of rapamycin signaling pathway; ULK1: Unc-51 like kinase 1.

the positive expression of related markers (Figure 1D-G). We found that XJZ decreased the positive expression of Dys and IM markers Ki-67 and CDX-2 in gastric mucosa tissues in a dose-dependent manner (Figure 1D-G).

We next investigated the protective effect of XJZ on the gastric mucosa and its effect on the liver and kidney. The results revealed that XJZ reduced serum MDA levels and increased SOD levels in rats, as well as reduced the levels of ALT and Cr, which are serum markers of liver and kidney injury (Figure 1H and I). These results indicate that XJZ can improve the general condition of rats, inhibit IM and Dys, has an antioxidant damage effect, has some protective effects on gastric mucosa, and has little effect on the liver and kidney of rats, making it an ideal drug for inhibiting GPL.

XJZ inhibits autophagy of gastric mucosal cells in GPL rats

As a biological process throughout GPL, autophagy maintains the survival of IM and Dys cells and destroys normal gastric mucosal cells. These effects promote GPL progression. Therefore, we examined autophagy levels in the gastric mucosal cells of rats. Transmission electron microscopy revealed that the formation of crescent-shaped autophagosomes, double-membrane autophagic vesicles, and the number of autolysosomes in the gastric mucosal tissue in the model group were significantly increased



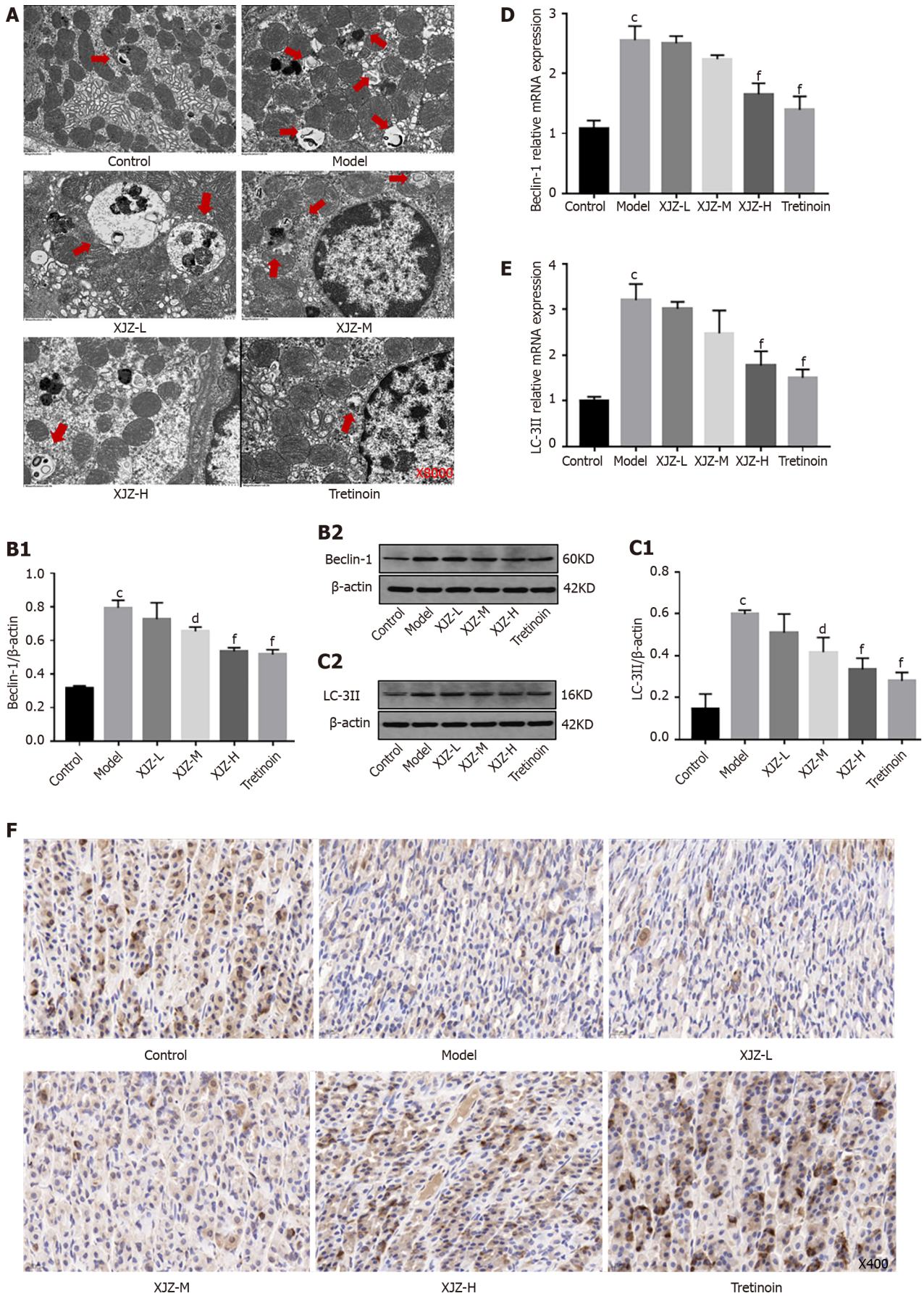
DOI: 10.4251/wjgo.v15.i3.464 Copyright ©The Author(s) 2023.

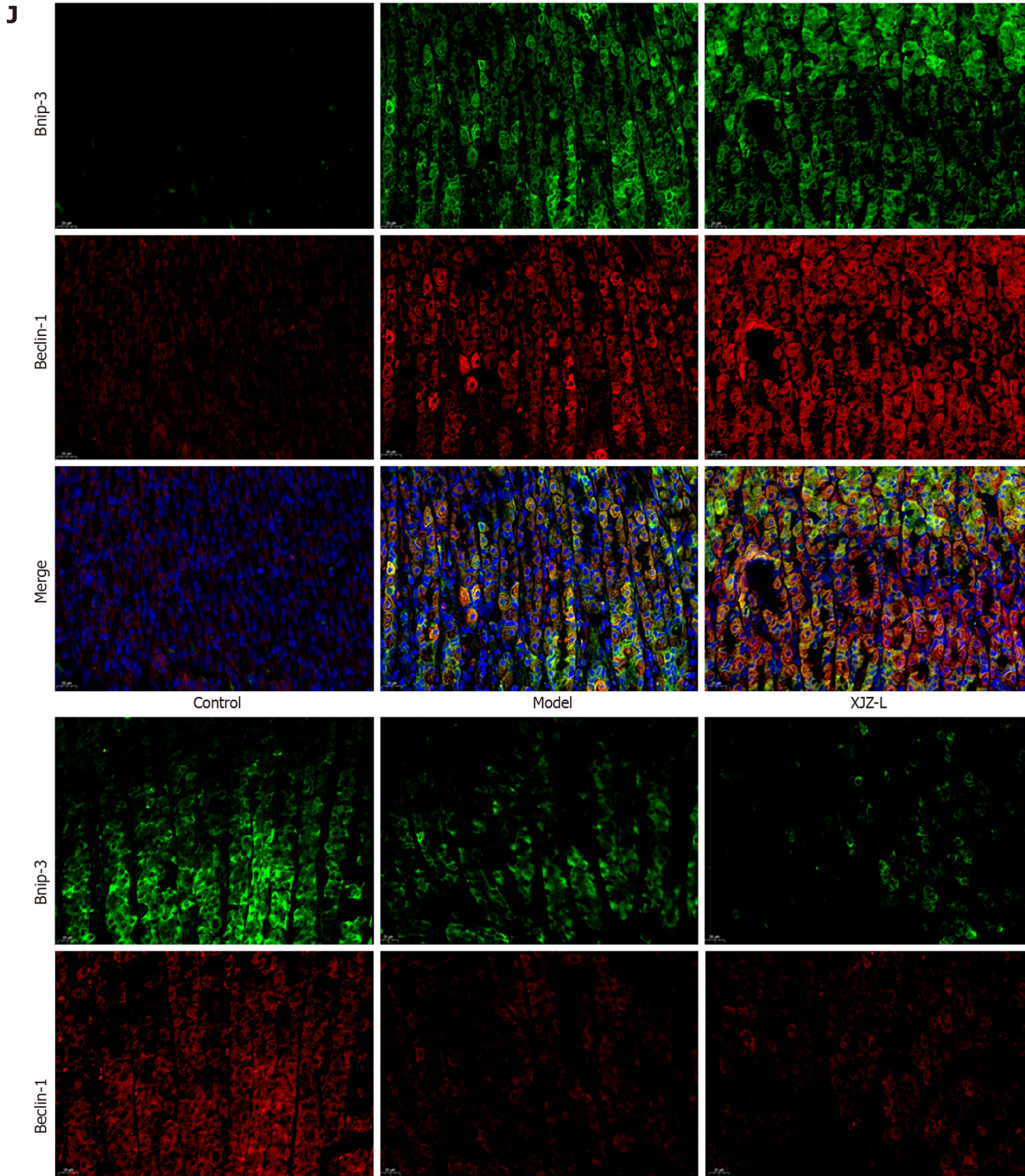
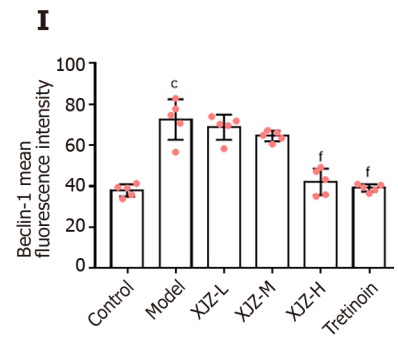
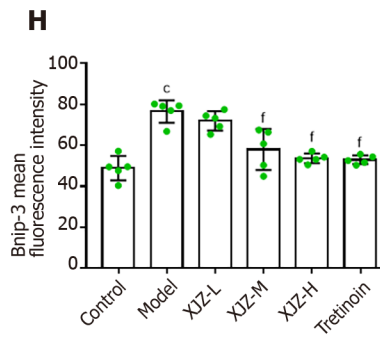
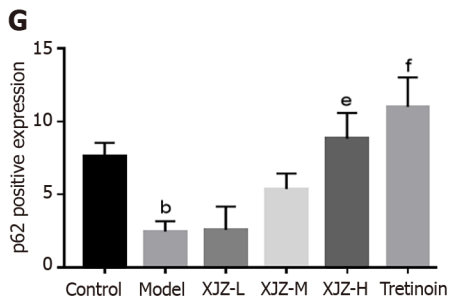
Figure 2 Result of the high-performance liquid chromatography method coupled with triple-quadrupole tandem mass spectrometry assays of the chemical composition of Xiaojianzhong decoction. A: High-performance liquid chromatography chromatogram; B-F: Compounds contained in Xiaojianzhong decoction.

compared with those in the control group, whereas XJZ reduced the formation of all the above autophagy-related structures in the gastric mucosal tissue (Figure 3A). Furthermore, we detected the related proteins involved in autophagy. The results showed that XJZ decreased Beclin-1 and LC-3II protein expressions and transcript levels in a dose-dependent manner (Figure 3B-E), increased p62 expression in gastric mucosal tissues (brown) (Figure 3F and G), and reduced the co-expression of Bnip-3 and Beclin-1 in the gastric mucosa (Figure 3H-J). These findings indicate that XJZ can inhibit autophagosome formation and autophagy level in GPL gastric mucosal tissues.

XJZ promotes the activation of the PI3K/AKT/mTOR signaling pathway to inhibit autophagy

The PI3K/AKT/mTOR signaling pathway is a classical pathway that regulates autophagy, and its inhibition activates autophagy[12]. We found that XJZ promoted PI3K, AKT, mTOR protein phosphorylation, and mRNA expressions in a dose-dependent manner (Figure 4), suggesting that it inhibits autophagy by activating the PI3K/AKT/mTOR signaling pathway. However, autophagy is also regulated by other mechanisms; for example, hypoxia is an important trigger of autophagy. Many studies have confirmed that the inflammatory state of the GPL gastric mucosa increases cellular oxygen consumption and creates a hypoxic microenvironment. Therefore, we explored the effect of XJZ on gastric mucosal hypoxia.





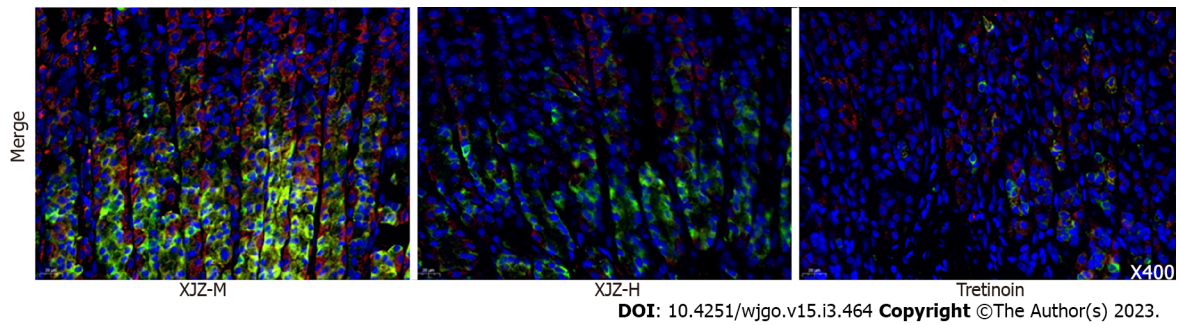


Figure 3 Effects of Xiaojianzhong decoction on autophagy of gastric mucosal epithelial cells in N-methyl-N'-nitro-N-nitrosoguanidine-induced gastric precancerous lesions rats. A: Observation of autophagy in rat gastric epithelial cells by transmission electron microscope (the red arrows in the figure are autophagosomes or autophagolysosomes); B and C: Western blot analysis was performed to detect BCL2-interacting protein 1 (Beclin-1), microtubule associated protein 1 light chain 3 (LC-3) II protein expression ($n = 3$); D and E: Beclin-1, LC-3II mRNA expression was determined using real-time polymerase chain reaction analysis ($n = 3$); F and G: p62 expression was determined using immunohistochemistry ($n = 5$); p62 positive score was determined using Image J; H-J: B cell lymphoma/leukemia-2 and adenovirus E1B19000 interacting protein 3 (Bnip-3), Beclin-1 proteins expression was determined using immunofluorescence ($n = 5$); Bnip-3, Beclin-1 proteins positive score was determined using ImageJ. Data are expressed as mean \pm SD. ^a $P < 0.05$, ^b $P < 0.01$, ^c $P < 0.001$ vs control group; ^d $P < 0.05$, ^e $P < 0.01$, ^f $P < 0.001$ vs model group. XJZ-L: Low dose of Xiaojianzhong decoction; XJZ-M: Middle dose of Xiaojianzhong decoction; XJZ-H: High dose of Xiaojianzhong decoction; Beclin-1: BCL2-interacting protein 1; LC-3: Microtubule associated protein 1 light chain 3.

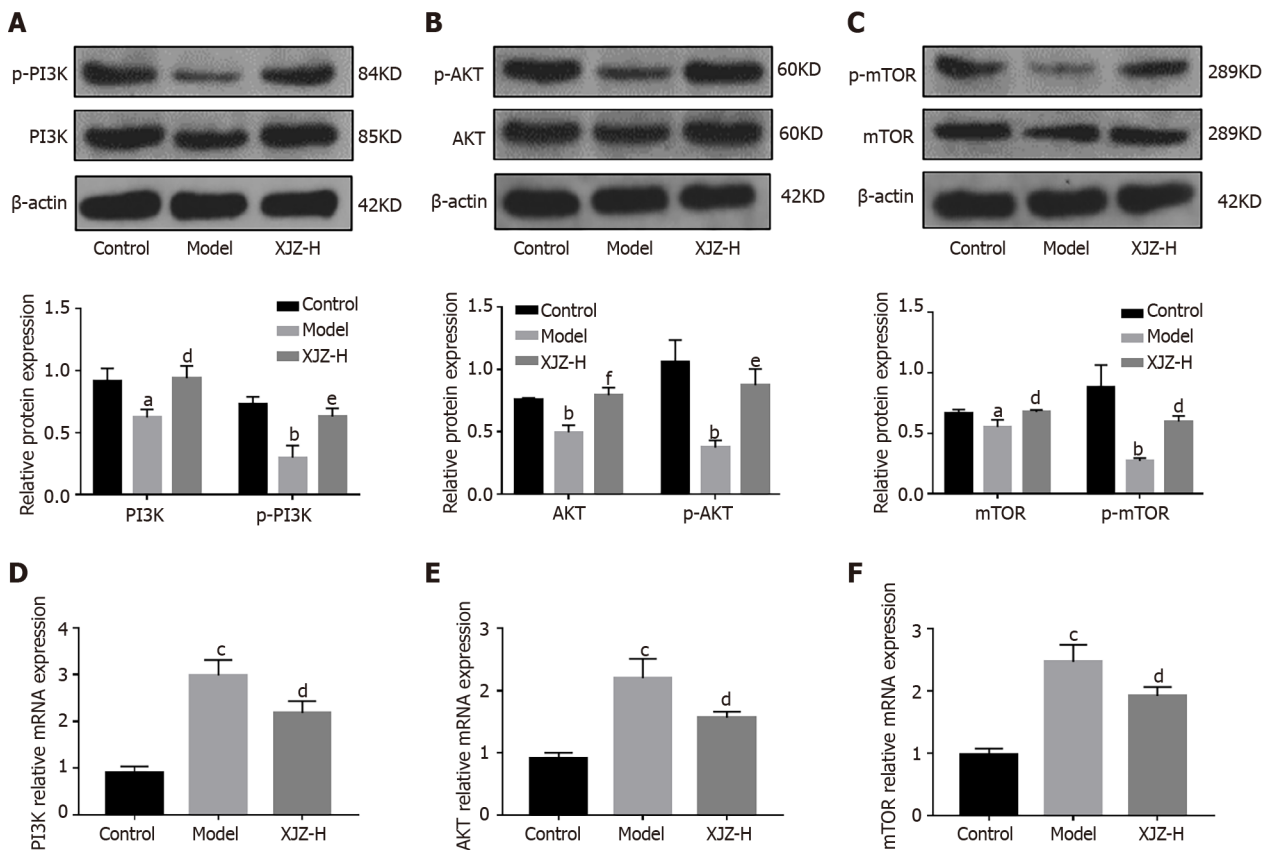


Figure 4 Xiaojianzhong decoction up-regulates phosphatidylinositol 3-kinase/protein kinase B/mammalian target of rapamycin signaling pathway in N-methyl-N'-nitro-N-nitrosoguanidine-induced gastric precancerous lesions rats. A-C: Western blot analysis was performed to detect phosphorylated-phosphatidylinositol 3-kinase (p-PI3K), phosphorylated-protein kinase B (p-AKT), and phosphorylated-mammalian target of rapamycin (p-mTOR) protein expression ($n = 3$); D-F: PI3K, AKT, and mTOR mRNA expression was determined using real-time polymerase chain reaction analysis ($n = 3$). Data are expressed as mean \pm standard deviation. ^a $P < 0.05$, ^b $P < 0.01$, ^c $P < 0.001$ vs control group; ^d $P < 0.05$, ^e $P < 0.01$, ^f $P < 0.001$ vs model group. XJZ-L: Low dose of Xiaojianzhong decoction; XJZ-M: Middle dose of Xiaojianzhong decoction; XJZ-H: High dose of Xiaojianzhong decoction.

XJZ ameliorates gastric mucosal hypoxia to inhibit autophagy and glycolysis in GPL rats

The hypoxic microenvironment of GPL gastric mucosa promotes the stable expression of HIF-1 α , a marker of tissue hypoxia, and HIF-1 α can specifically induce autophagy under hypoxia[13]. To investigate whether XJZ could inhibit autophagy by improving gastric mucosal hypoxia, we examined

the activation of HIF-1 α and related autophagic pathways. The results revealed that XJZ dose-dependently inhibited HIF-1 α and Bnip-3 protein and mRNA expressions (Figure 5A-D) and reduced the co-expression of HIF-1 α and Bnip-3 protein in the gastric mucosa (Figure 5E-G). Thus, XJZ can ameliorate hypoxia of gastric mucosa in the GPLs and inhibit the activation of the HIF-1 α /Bnip-3 signaling pathway, thereby decreasing autophagy.

In addition to regulating autophagy, hypoxia also causes abnormal glucose metabolism. HIF-1 α can directly promote the transcription of glycolytic target genes and change the metabolic mode from aerobic oxidative phosphorylation to anaerobic glycolysis, thereby accelerating the cellular energy supply and promoting dysplastic cell proliferation, and GPL deterioration[14]. We observed that XJZ dose-dependently reduced the co-expression of HIF-1 α and CD147 (Figure 6A-C), which assists in lactate transport, in the rat gastric mucosa and inhibited the mRNA transcription of Monocarboxylate transporter (MCT1), MCT4, and CD147 (Figure 6D-F). Immunohistochemistry results revealed that XJZ promoted the expression of glycolysis co-repressor SIRT6 in the gastric mucosa, while the structure of gastric mucosal glands returned to normal (Figure 6G and H). Therefore, gastric mucosal hypoxia and HIF-1 α expression, as important factors of glycolysis initiation, may be regulated by XJZ, thereby inhibiting glycolysis and preventing GPL progression.

XJZ inhibits ULK1 activation to improve abnormal glucose metabolism and autophagy

To further elucidate the underlying mechanism of glycolysis inhibition by XJZ, we next investigated the effect of XJZ on the activation of ULK1, a signaling molecule involved in initiating glycolysis. Our experiments revealed that XJZ effectively inhibited the transcriptional level and expression of ULK1 in gastric mucosa (Figure 7A-C), suggesting that the improvement of glucose metabolism by XJZ may be related to ULK1 inhibition.

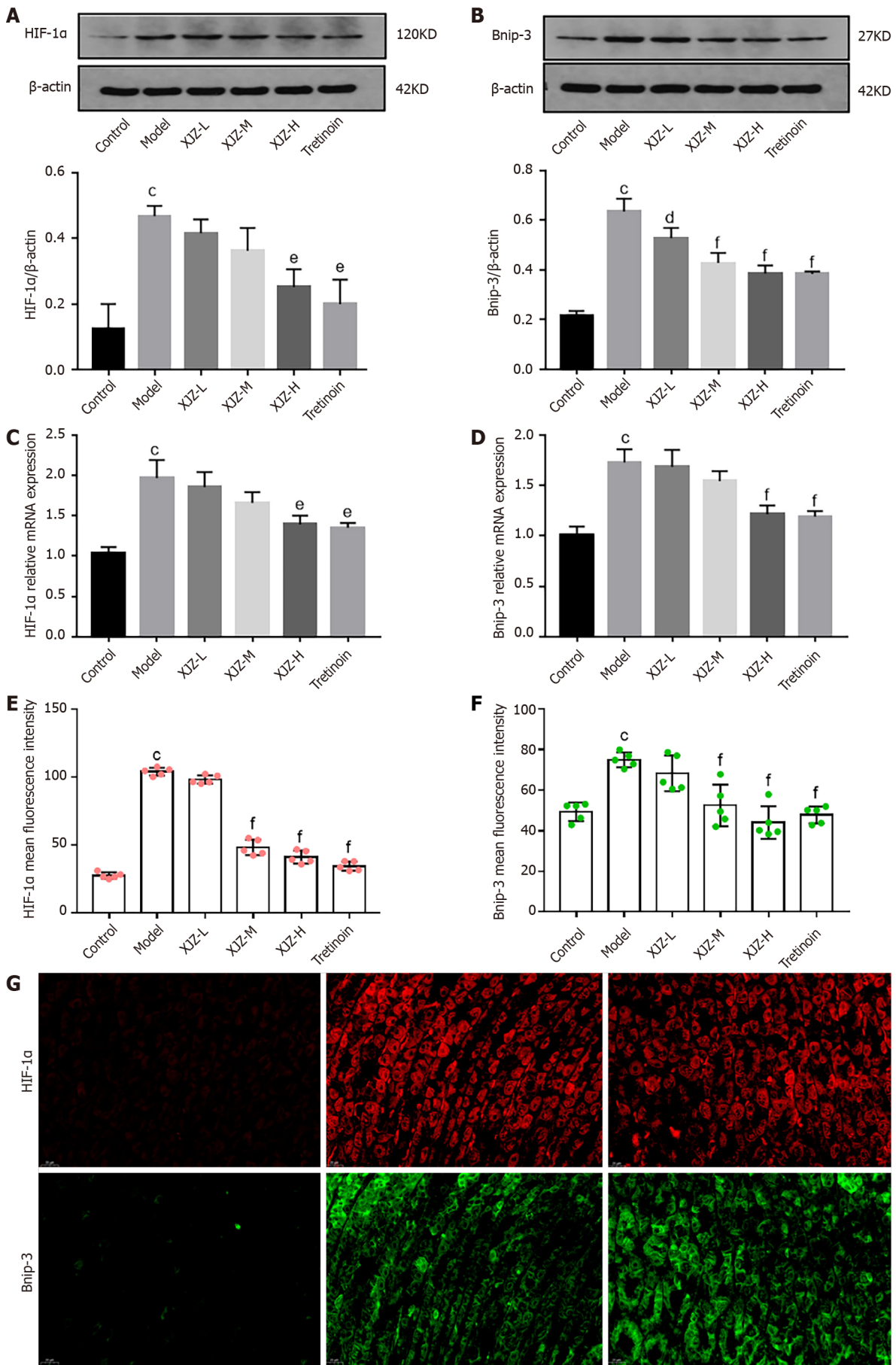
Notably, in addition to affecting glycolysis, ULK1 activation also promotes autophagy initiation. The p53 nucleoprotein upstream of ULK1 promotes the phosphorylation of the ULK1 Ser-317 and Ser-555 sites by activating AMPK, thus activating autophagy[15,16]. We next examined the phosphorylation levels of ULK1 autophagy-related sites and the p53/AMPK signaling pathway. The results showed that XJZ inhibited the phosphorylation of p53 nucleoprotein, AMPK, and ULK1 Ser-317 and Ser-555 sites in a dose-dependent manner (Figure 7D-G) and reduced p53 expression in gastric mucosa (Figure 7H-I). The above results suggest that XJZ may also inhibit autophagy by regulating the phosphorylation levels of the p53/AMPK pathway and ULK1 autophagy-related sites (Figure 8).

DISCUSSION

GPL is inevitable for the occurrence and development of GC. In the past few decades, the incidence of GPLs has been increasing worldwide, predominantly in East Asia, South America, and Central Europe [17,18]. Although the importance of preventing and treating GPL has been clarified, many patients are unable to receive timely and effective treatment, eventually leading to GC. In this study, we reported that the traditional Chinese herbal medicine XJZ has a preventive and therapeutic effect on GPLs and that the possible underlying mechanism is related to inhibiting autophagy and improving the hypoxic environment of gastric mucosa and abnormal glucose metabolism.

When GPL occurs, normal gastric mucosal cells are gradually replaced by IM and Dys cells, a large amount of acidic mucus is secreted, and CDX-2 and Ki-67 are abnormally expressed[19,20]. CDX-2 is a nuclear transcription factor that is mainly expressed in the small intestine and colon. When it is ectopically expressed in the gastric mucosa, it marks the occurrence of IM[21]. Ki-67 is closely related to cell proliferation and ribosome transcription and is often used to assess the level of tumor proliferation. If the gastric mucosa expresses Ki-67, it indicates the occurrence of Dys[22]. XJZ improved the general condition of GPL rats, reduced the degree of gastric mucosal injury and pathology, inhibited CDX-2 and Ki-67 expressions in gastric mucosa, adjusted serum MDA and SOD levels associated with oxidative stress injury, and protected the gastric mucosal barrier. All these pathomechanisms may be related to the inhibition of autophagy by XJZ.

Autophagy is an essential and highly conserved biological process that occurs in various human cells. Autophagy is activated during the GPLs by factors such as hypoxia and signaling molecule disorders and affects the pathological process of GPL. However, few studies have analyzed the role of autophagy in GPLs. Autophagy can remove harmful factors from IM and Dys cells through lysosomes. The increase in its level not only maintains the stability of the intracellular environment and cell survival in dysplastic cells but also exacerbates the gastric mucosal injury and genomic disorders by promoting the autophagic death of normal cells[23,24]. Thus, uncontrolled autophagy further promotes GPL deterioration. Bnip-3 binds to and activates LC3, which exists in two forms: LC3-I and LC3-II, and LC3-II is involved in autophagosome formation, together with autophagy-related protein Beclin-1[25]. In addition, LC3-II can bind the autophagy substrate p62 to autophagosomes to promote the formation and degradation of autophagy-lysosomes[26]. This degradation also degrades the "task-completed" p62 to decrease its expression, so the p62 Level can reflect the autophagy level. XJZ can reduce the formation of autophagosomes and autolysosomes, inhibit the protein expressions and transcription levels of Bnip-



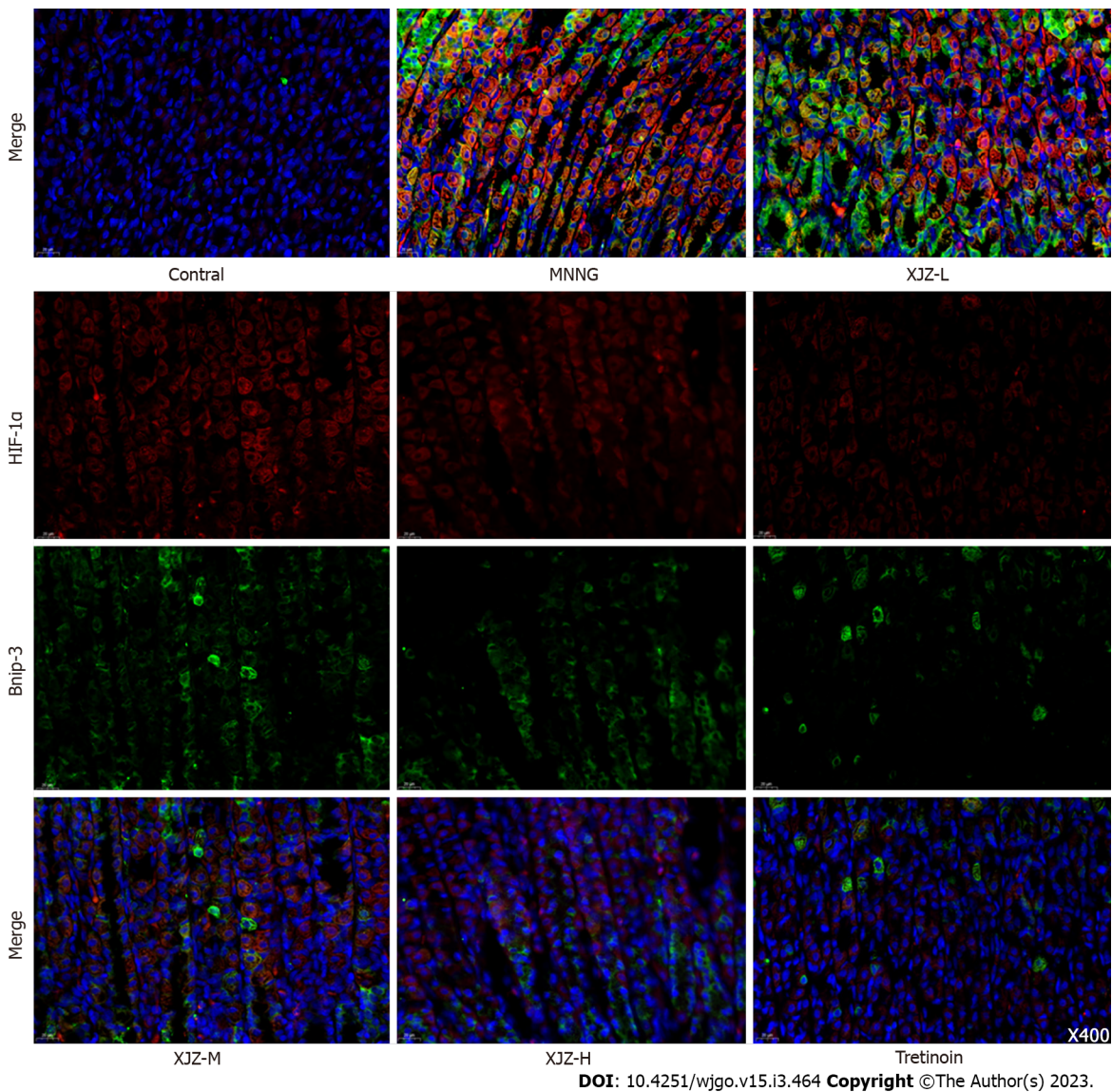
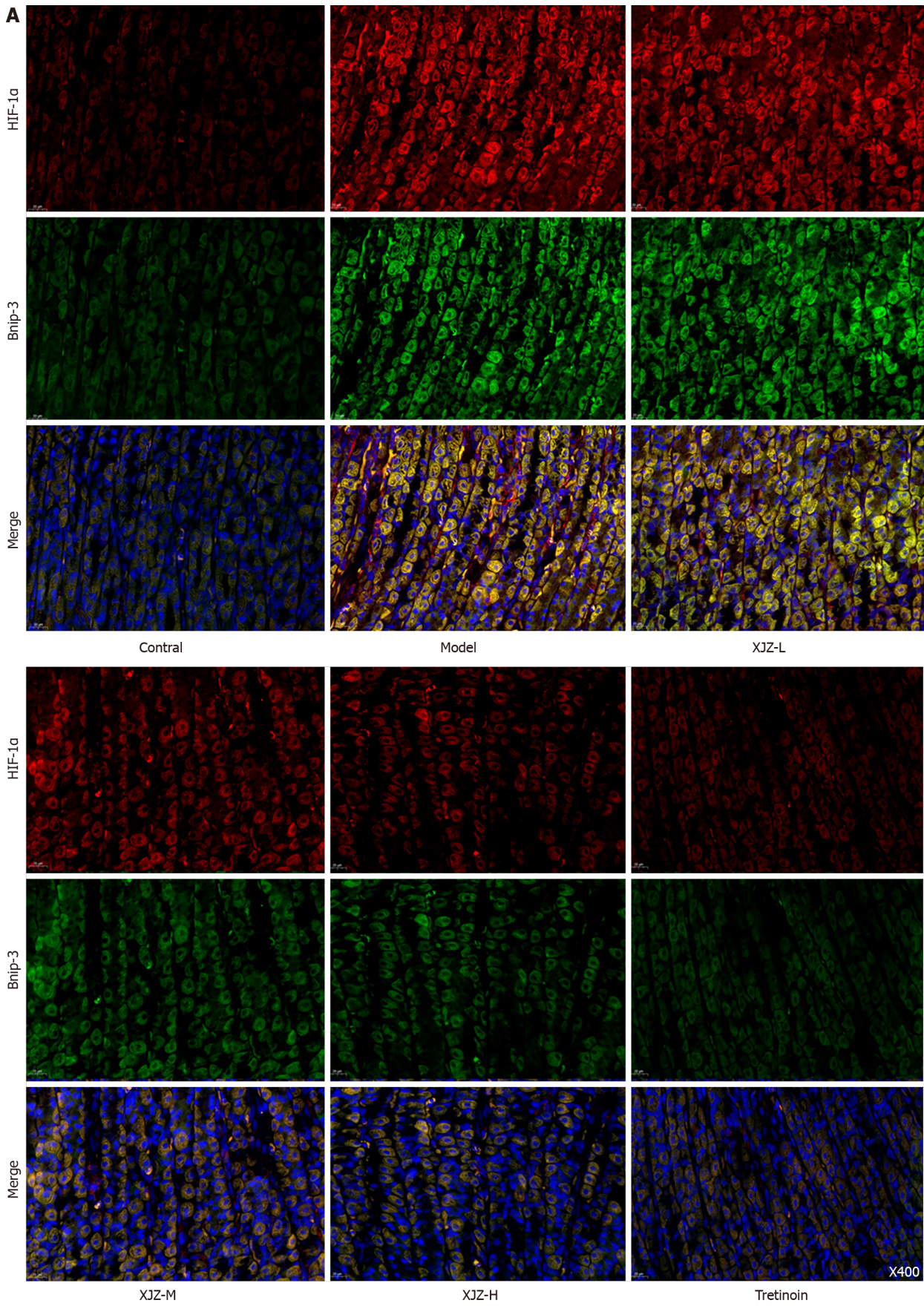


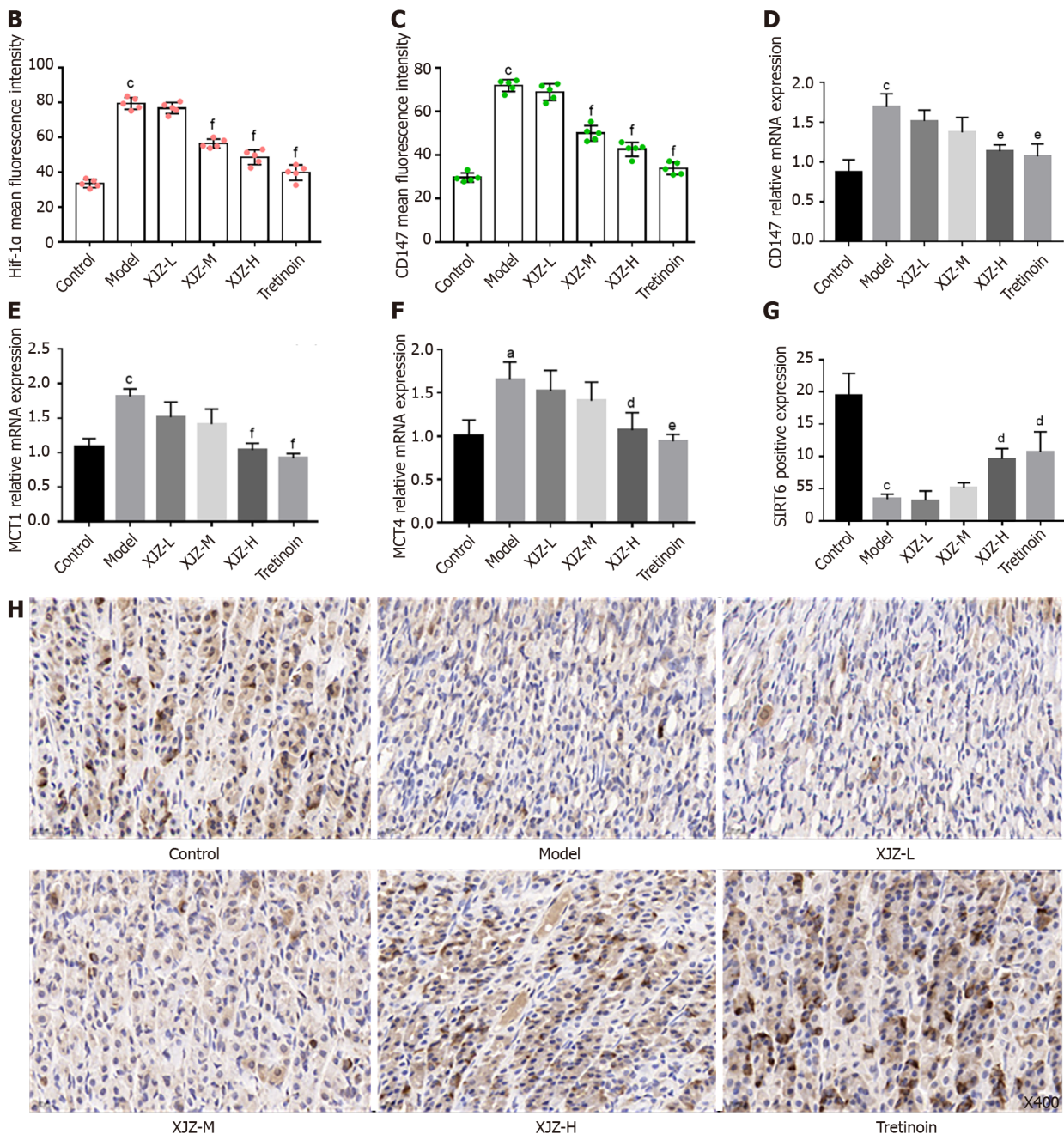
Figure 5 Effects of Xiaojianzhong decoction on gastric mucosal hypoxia in N-methyl-N'-nitro-N-nitrosoguanidine-induced gastric precancerous lesions rats. A and B: Western blot analysis was performed to detect hypoxia-inducible factor 1 α (HIF-1 α), E1B19000 interacting protein 3 (Bnip-3) protein expression ($n = 3$); C and D: HIF-1 α , Bnip-3 mRNA expression was determined using real-time polymerase chain reaction analysis ($n = 3$); E-G: Hypoxia-induced autophagy-related protein HIF-1 α , Bnip-3 expression was determined using immunofluorescence ($n = 5$); HIF-1 α , Bnip-3 proteins positive score was determined using Image J. Data are expressed as mean \pm SD. ^a $P < 0.05$, ^b $P < 0.01$, ^c $P < 0.001$ vs control group; ^d $P < 0.05$, ^e $P < 0.01$, ^f $P < 0.001$ vs model group. XJZ-L: Low dose of Xiaojianzhong decoction; XJZ-M: Middle dose of Xiaojianzhong decoction; XJZ-H: High dose of Xiaojianzhong decoction; HIF-1 α : Hypoxia-inducible factor 1 α ; Bnip-3: B cell lymphoma/Leukemia-2 and adenovirus E1B19000 interacting protein 3.

3, Beclin-1, and LC-3II; and promote p62 expression in the gastric mucosa of rats with GPL, suggesting that XJZ has a rather comprehensive inhibitory effect on autophagy.

The PI3K/Akt/mTOR pathway is a classical autophagy regulatory pathway. PI3K activation promotes AKT activation, which further binds AKT to the TSC1/2 complex to activate mTOR. The mTOR can form two complexes, mTORC1 and mTORC2. The mTORC1 promotes the phosphorylation of the ribosomal protein P70S6K, and the phosphorylated P70S6K, in turn, activates mTOR to downregulate the expression of ULK1, which is involved in the initiation of autophagy, thereby inhibiting autophagy[27,28]. XJZ can increase the protein phosphorylation and transcription levels of PI3K, Akt, and mTOR in the gastric mucosa, which may be one of the potential mechanisms by which XJZ inhibits autophagy. In addition to the PI3K/Akt/mTOR pathway, hypoxia, a characteristic state of GPL gastric mucosa, also affected the initiation of autophagy.

The gastric mucosa of GPL is filled with a large number of inflammatory cells and inflammatory factors, and their high metabolic levels increase oxygen consumption, leading to gastric mucosal hypoxia and promoting the expression of the hypoxia adaptation regulator HIF-1 α [29]. HIF-1 α can bind to the autophagy-associated protein Bnip-3 through the hormone response element (HRE) binding domain to initiate autophagy[30], so the regulation of HIF-1 α is crucial for inhibiting autophagy. Several studies have demonstrated that HIF-1 α is activated in the hypoxic microenvironment of GPL[31,32],



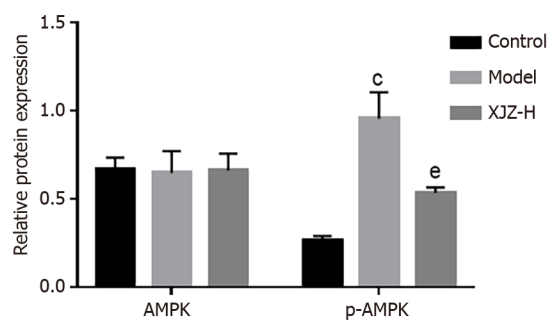
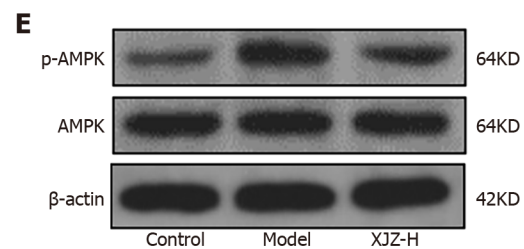
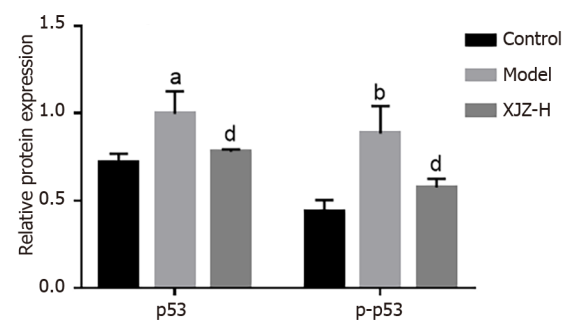
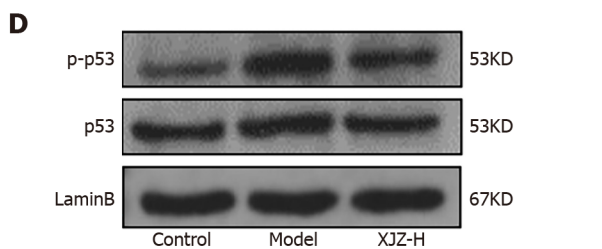
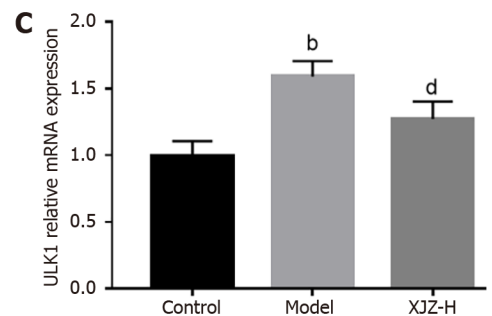
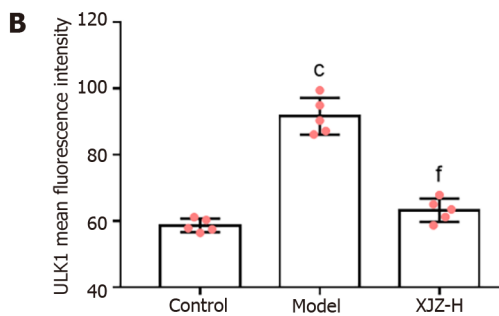
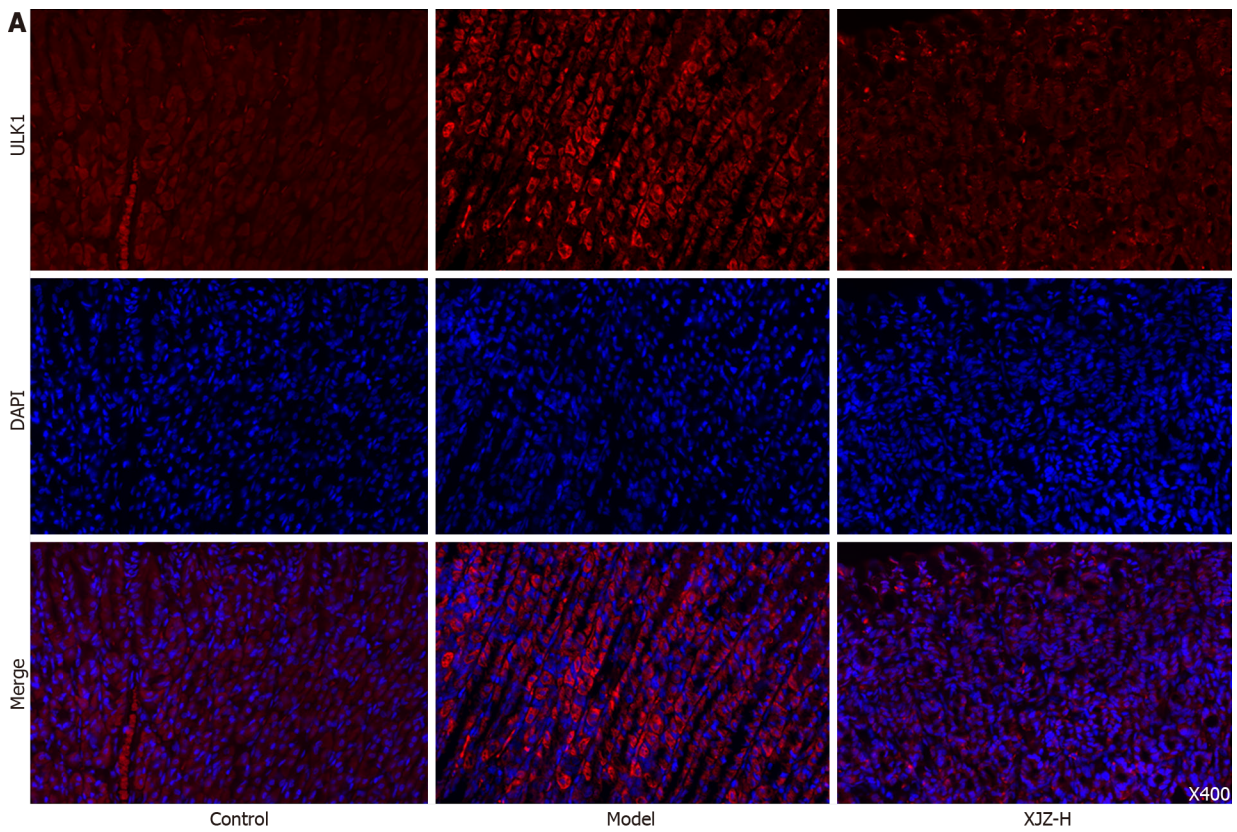


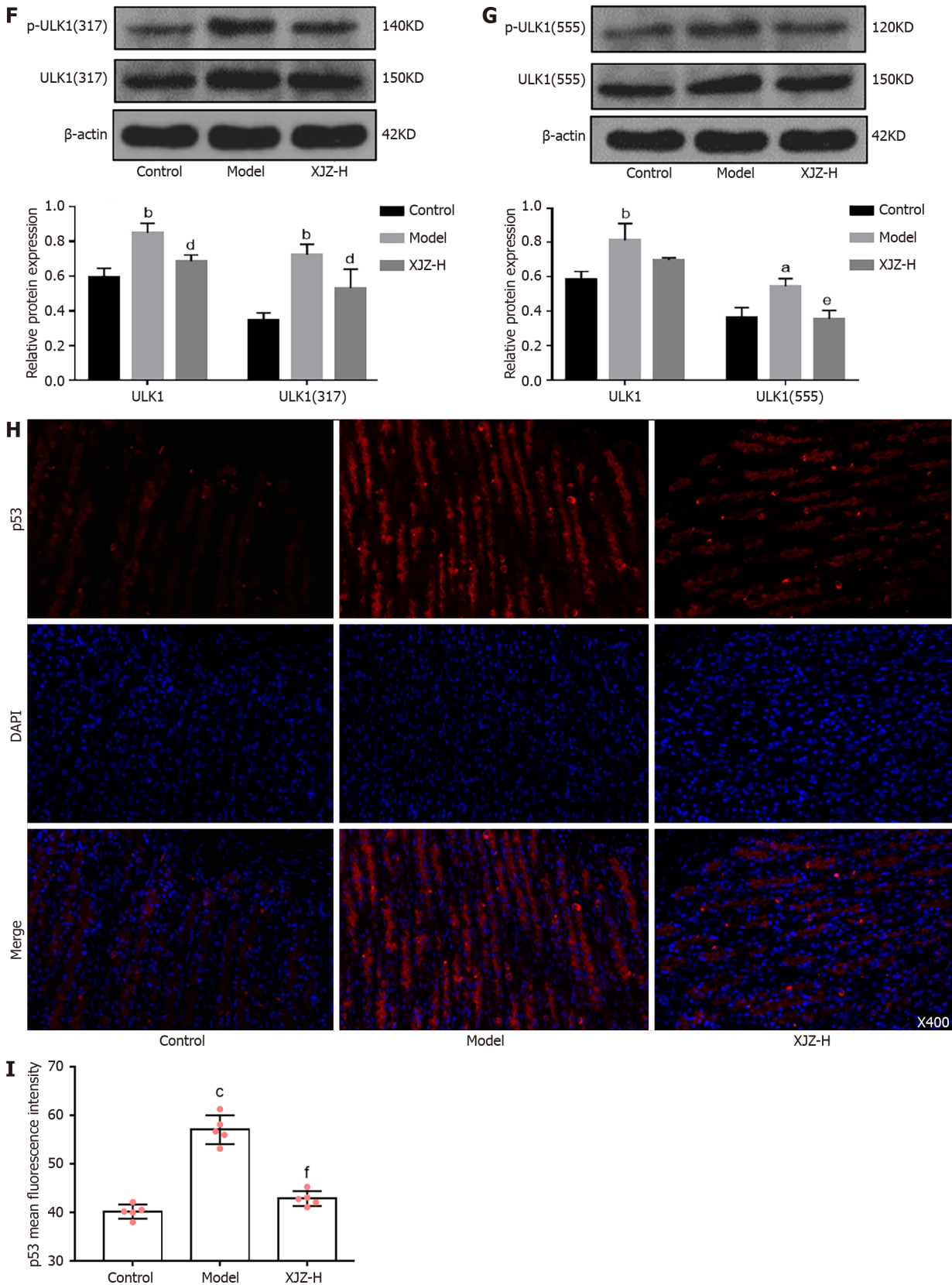
DOI: 10.4251/wjgo.v15.i3.464 Copyright ©The Author(s) 2023.

Figure 6 Effects of Xiaojianzhong decoction on hypoxia-induced glycolysis in gastric mucosal epithelial cells. A-C: Hypoxia-induced glycolysis-related protein hypoxia-inducible factor 1 α (HIF-1 α), CD147 expression was determined using immunofluorescence ($n = 5$); HIF-1 α , CD147 proteins positive score was determined using Image J; D-F: CD147, monocarboxylate transporter (MCT1), and MCT4 mRNA expression was determined using real-time polymerase chain reaction analysis ($n = 3$); G and H: Sirtuin 6 (SIRT6) expression was determined using immunohistochemistry ($n = 5$); SIRT-6 positive score was determined using Image J. Data are expressed as mean \pm SD. ^a $P < 0.05$, ^b $P < 0.01$, ^c $P < 0.001$ vs control group; ^d $P < 0.05$, ^e $P < 0.01$, ^f $P < 0.001$ vs model group. XJZ-L: Low dose of Xiaojianzhong decoction; XJZ-M: Middle dose of Xiaojianzhong decoction; XJZ-H: High dose of Xiaojianzhong decoction; HIF-1 α : Hypoxia-inducible factor 1 α ; MCT: Monocarboxylate transporter.

consistent with our results. The increase in HIF-1 α protein and transcript levels in the gastric mucosa of rats in the MNNG group indicated that the gastric mucosa was in a hypoxic state. After the intervention with XJZ, the protein expressions and transcription levels of HIF-1 α and Bnip-3, as well as their co-expression in the gastric mucosa were reduced, suggesting that XJZ can improve gastric mucosal hypoxia and may inhibit autophagy initiation for this reason.

Interestingly, we observed that XJZ also improved abnormal glucose metabolism in GPL gastric mucosal cells by inhibiting the expression of HIF-1 α . In addition to the effect on autophagy, HIF-1 α also promotes the shift of cellular energy metabolism from oxidative phosphorylation to glycolysis. Glycolysis often occurs in a hypoxic state, and the stable expression of HIF-1 α promotes the transcription of glycolytic target genes, which eventually generate ATP and lactate through a series of





DOI: 10.4251/wjgo.v15.i3.464 Copyright ©The Author(s) 2023.

Figure 7 Xiaojianzhong decoction inhibited Unc-51 Like kinase 1 and p53/AMP-activated protein kinase pathway in N-methyl-N'-nitro-N-nitrosoguanidine-induced gastric precancerous lesions rats. A and B: Unc-51 like kinase 1 (ULK1) and p53 protein expression was determined using immunofluorescence ($n = 5$); ULK1, p53 proteins positive score was determined using Image J; C: ULK1 mRNA expression was determined using real-time polymerase chain reaction analysis ($n = 3$); D-G: Western blot analysis was performed to detect p-p53, p-AMP-activated protein kinase, p-ULK1 (Ser555), and p-ULK1 (Ser317) protein expression ($n = 3$); H and I: ULK1 and p53 protein expression was determined using immunofluorescence ($n = 5$). Data are expressed as

mean \pm SD. ^a $P < 0.05$, ^b $P < 0.01$, ^c $P < 0.001$ vs control group; ^d $P < 0.05$, ^e $P < 0.01$, ^f $P < 0.001$ vs model group. XJZ-L: Low dose of Xiaojianzhong decoction; XJZ-M: Middle dose of Xiaojianzhong decoction; XJZ-H: High dose of Xiaojianzhong decoction; ULK1: Unc-51 like kinase 1.

metabolic reactions[33]. Glycolysis is common in a variety of tumor diseases, including GC. Its rapid energy production meets the energy demand for tumor cell growth and proliferation, while the increase in effluent lactate also promotes tumor progression[34,35]. CD147 activation assists MCT1 and MCT4 in outward lactate transport and the increased accumulation of extracellular lactate forms an acidic environment suitable for tumor growth[36]. In addition, low SIRT6 expression during high glycolytic activity impedes the deacetylation of H3K9 and promotes the transcription of glycolysis-related genes [37]. Our experiments revealed that XJZ reduced the co-expression of HIF-1 α /CD147 in gastric mucosa and the transcription levels of MCT1, MCT4, and CD147. Immunohistochemistry results showed that the SIRT6 expression in the gastric mucosa was upregulated with the increase of XJZ dose and the GPL-related pathological manifestations were ameliorated. These suggest that XJZ may decrease abnormal glucose metabolism by preventing gastric mucosa from hypoxia. Glycolysis has been a hotspot in the research of tumor-related diseases in recent years, but its effects on GPL remain unclear. Our results indicated the adverse effects of higher glycolysis level on GPL and the culprit may be closely related to gastric mucosal hypoxia. In addition to hypoxia, the initiation of glycolysis is also affected by various factors, so we continued to explore the potential mechanism of XJZ in regulating glycolysis in gastric mucosal cells.

ULK1 is an important signaling molecule that affects glycolysis level and is highly expressed in the gastric mucosa during the GPL stage. More specifically, it improves the glycolysis level by promoting the transcription of key glycolysis enzyme genes such as hexokinase 2 (HK2) and phosphofructokinase-1[38]. It has previously been revealed that XJZ reduces the expression and transcription levels of ULK1 in gastric mucosa, which suggests that the inhibition of ULK1 expression could be a potential mechanism by which XJZ regulates the glycolysis level. As mentioned above, ULK1 is also involved in the regulation of autophagy, principally due to the different regulatory roles of its upstream PI3K/AKT/mTOR and p53/AMPK signaling pathways. Notably, p53 is an important metabolic regulator known to affect both autophagy and glycolysis in multiple ways[39]. On the one hand, the activation of nucleoprotein, p53, prompts AMPK to phosphorylate the 317 and 555 sites of ULK1, thereby activating autophagy[40,41]. It has also been determined that p53 can induce mitochondrial autophagy by increasing the Bnip-3 level[42] or promote its target, TP53INP1, to bind the LC-3 and Autophagy-related protein 8 (ATG8) proteins, leading to the excessive activation of autophagy or even autophagic cell death[43]. On the other hand, p53 activates cyclooxygenase 2 (COX-2) to promote the production of reactive oxygen species (ROS), while ROS, as an important product of glycolysis, stabilizes the expression of HIF-1 α and maintains glycolytic activity[44]. In the present study, we focused on examining the effects of XJZ on the activation of the p53/AMPK pathway and ULK1 autophagy-related sites. Our results revealed that XJZ inhibited the expression of p53 in gastric mucosa and the phosphorylation of the nucleoprotein p53, AMPK, and the ULK1 317 and 555 sites. This indicates that the inhibition of the p53/AMPK signaling pathway and the phosphorylation of the ULK1 317 and 555 sites may also represent a potential mechanism for the regulation of autophagy by XJZ in GPL. Moreover, the inhibition of ULK1 and the nucleoprotein p53 by XJZ may be involved in the dual regulation of autophagy and glycolysis in GPL. In addition, this result suggests that the inhibition of autophagy by XJZ may stem from the co-regulation of the PI3K/AKT/mTOR and p53/AMPK/ULK1 pathways.

Notably, a recent study on *Escherichia coli* found that HIF-1 α activation can also activate autophagy by promoting ULK1 expression[45]; however, this result has not been confirmed in GPL-related studies. Our data showed that XJZ inhibited the expressions of HIF-1 α and ULK1 in the gastric mucosa of GPL rats. It is speculated that XJZ may also affect autophagy by ameliorating gastric mucosal hypoxia to downregulate ULK1 expression.

Little is currently known about the effects of the main components of XJZ on both autophagy and glycolysis in gastric mucosal cells. Some prior studies have determined that the cinnamaldehyde found in XJZ can inhibit autophagy through the AMPK/mTOR/ULK1 signaling pathway in esophageal cancer cells, which suggests the possibility of adjusting autophagy to a level that can maintain intracellular homeostasis[46]. Moreover, paeoniflorin has been found to inhibit the autophagy level by inhibiting the expression of Beclin-1 and LC-3II in cardiomyocytes, thereby protecting the cardiomyocytes[47]. The 6-gingerol has been observed to inhibit autophagy by targeting the Notch signaling pathway in order to block breast cancer cell growth[48]. In addition, licorice chalcone A was found to inhibit the glycolysis level through the PI3K/AKT signaling pathway in mouse melanoma B16F10 cells[49]. These studies of the main components of XJZ in other disease models may provide useful insights into the specific components of XJZ that act in gastric mucosal cells.

In the present study, we determined that XJZ was able to effectively prevent the progression of MNNG-induced GPL in rats, and it may prevent the further deterioration of GPL by regulating autophagy, glycolysis, and gastric mucosal hypoxia. However, this study did not verify the relevant signaling molecules and pathways to further clarify the specific mechanism of XJZ in the treatment of

epithelial cells, and provide a theoretical basis for the clinical prevention and treatment of GPL.

Research methods

Using the N-methyl-N'-nitro-N-nitrosoguanidine (MNNG) compound modeling method to construct a model of gastric precancerous lesions in rats, intervene with XJZ, and use a variety of methods to detect the effects of XJZ on autophagy, glycolysis and gastric precancerous lesions in rats.

Research results

The treatment of XJZ can promote the weight gain of rats and improve the pathological manifestations of GPL-related tissues; the formation of autophagosomes and autolysosomes in gastric tissue is reduced, and the expressions of B cell lymphoma/leukemia-2 and adenovirus E1B19000 interacting protein 3, moesin-like BCL2-interacting protein 1, and microtubule associated protein 1 light chain 3 are reduced. The expression of p62 increased, and the level of autophagy was fully inhibited. XJZ inhibited the level of autophagy by activating the phosphatidylinositol 3-kinase/protein kinase B/mammalian target of rapamycin (PI3K/AKT/mTOR) pathway; while improving gastric mucosal hypoxia, it could also inhibit autophagy and improve abnormal glucose metabolism in gastric mucosal cells. XJZ inhibited the expression of Unc-51 Like kinase 1 (ULK1) to improve abnormal glucose metabolism in gastric mucosa, and prevented the increase of autophagy level by inhibiting p53/AMP-activated protein kinase (AMPK) pathway and ULK1 Ser317555 phosphorylation.

Research conclusions

Xiaojianzhong Decoction has a therapeutic effect on MNNG-induced gastric precancerous lesions, which may be achieved through the joint regulation of PI3K/AKT/mTOR, p53/AMPK/ULK1 signaling pathways and gastric mucosal hypoxia.

Research perspectives

This study mainly explores Xiaojianzhong Decoction regulates PI3K/AKT/mTOR, p53/AMPK/ULK1 signaling pathways and gastric mucosal hypoxia to improve gastric precancerous lesions in rats.

FOOTNOTES

Author contributions: Zhang JX performed the experiments, sample detection, data analysis and wrote the manuscript; Bao SC, Chen J, and Chen T helped with the performing and sample collection of the animal experiment; Yan SG, Li JT, Wei HL, and Zhou XY conceived and supervised the experiments and finalized the manuscript; all authors reviewed the manuscript.

Supported by the Shaanxi Science and Technology overall Planning and Innovation Project, No. 2016KTTSSF01-05; Key R & D projects in Shaanxi Province, No. 2022ZDLSF05-10; and Shaanxi University of Chinese Medicine Discipline Innovation Team Construction Project, No. 2019-YL-05.

Institutional animal care and use committee statement: All procedures involving animals were reviewed and approved by the Regulations for the Care and Use of Laboratory Animals in Shaanxi University of Chinese Medicine (Approval No. SCXK 2019-0004).

Conflict-of-interest statement: The authors declare that there is no conflict of interest in this study.

Data sharing statement: Technical appendix, statistical code, and dataset are available from the corresponding author at ysg2002. student@sina.com upon reasonable request.

ARRIVE guidelines statement: The authors have read the ARRIVE guidelines, and the manuscript was prepared and revised according to the ARRIVE guidelines.

Open-Access: This article is an open-access article that was selected by an in-house editor and fully peer-reviewed by external reviewers. It is distributed in accordance with the Creative Commons Attribution NonCommercial (CC BY-NC 4.0) license, which permits others to distribute, remix, adapt, build upon this work non-commercially, and license their derivative works on different terms, provided the original work is properly cited and the use is non-commercial. See: <https://creativecommons.org/licenses/by-nc/4.0/>

Country/Territory of origin: China

ORCID number: Jia-Xiang Zhang 0000-0003-1129-5708; Sheng-Chuan Bao 0000-0003-3742-0220; Juan Chen 0000-0002-5269-7239; Ting Chen 0000-0001-8877-3988; Hai-Liang Wei 0000-0001-7751-1368; Xiao-Yan Zhou 0000-0002-4204-7486; Jing-Tao Li 0000-0003-0417-9821; Shu-Guang Yan 0000-0003-4694-6718.

S-Editor: Chen YL

L-Editor: Filipodia

P-Editor: Yu HG

REFERENCES

- 1 **Wang S**, Kuang J, Li G, Huang G, Zheng L, Li J, Wang L. Gastric precancerous lesions present in Apc(Min/+) mice. *Biomed Pharmacother* 2020; **121**: 109534 [PMID: 31810128 DOI: 10.1016/j.biopha.2019.109534]
- 2 **Du Y**, Bai Y, Xie P, Fang J, Wang X, Hou X, Tian D, Wang C, Liu Y, Sha W, Wang B, Li Y, Zhang G, Shi R, Xu J, Huang M, Han S, Liu J, Ren X, Wang Z, Cui L, Sheng J, Luo H, Zhao X, Dai N, Nie Y, Zou Y, Xia B, Fan Z, Chen Z, Lin S, Li ZS; Chinese Chronic Gastritis Research group. Chronic gastritis in China: a national multi-center survey. *BMC Gastroenterol* 2014; **14**: 21 [PMID: 24502423 DOI: 10.1186/1471-230X-14-21]
- 3 **Escobar KA**, Cole NH, Mermier CM, VanDusseldorp TA. Autophagy and aging: Maintaining the proteome through exercise and caloric restriction. *Aging Cell* 2019; **18**: e12876 [PMID: 30430746 DOI: 10.1111/ace1.12876]
- 4 **Nassour J**, Radford R, Correia A, Fusté JM, Schoell B, Jauch A, Shaw RJ, Karlseder J. Autophagic cell death restricts chromosomal instability during replicative crisis. *Nature* 2019; **565**: 659-663 [PMID: 30675059 DOI: 10.1038/s41586-019-0885-0]
- 5 **Zeng JH**, Pan HF, Liu YZ, Xu HB, Zhao ZM, Li HW, Ren JL, Chen LH, Hu X, Yan Y. Effects of Weipixiao on Wnt pathway-associated proteins in gastric mucosal epithelial cells from rats with gastric precancerous lesions. *Chin J Integr Med* 2016; **22**: 267-275 [PMID: 25877463 DOI: CNKI:SUN:BXYY.0.2018-09-093]
- 6 **Panieri E**, Santoro MM. ROS homeostasis and metabolism: a dangerous liason in cancer cells. *Cell Death Dis* 2016; **7**: e2253 [PMID: 27277675 DOI: 10.1038/cddis.2016.105]
- 7 **Sabbah HN**. Targeting the Mitochondria in Heart Failure: A Translational Perspective. *JACC Basic Transl Sci* 2020; **5**: 88-106 [PMID: 32043022 DOI: 10.1016/j.jacbts.2019.07.009]
- 8 **Neto JGO**, Boechat SK, Romão JS, Pazos-Moura CC, Oliveira KJ. Treatment with cinnamaldehyde reduces the visceral adiposity and regulates lipid metabolism, autophagy and endoplasmic reticulum stress in the liver of a rat model of early obesity. *J Nutr Biochem* 2020; **77**: 108321 [PMID: 31869758 DOI: 10.1016/j.jnutbio.2019.108321]
- 9 **Bawadood AS**, Al-Abbasi FA, Anwar F, El-Halawany AM, Al-Abd AM. 6-Shogaol suppresses the growth of breast cancer cells by inducing apoptosis and suppressing autophagy via targeting notch signaling pathway. *Biomed Pharmacother* 2020; **128**: 110302 [PMID: 32505819 DOI: 10.1016/j.biopha.2020.110302]
- 10 **Herrman TJ**, Hoffmann V, Muiruri A, McCORMICK C. Aflatoxin Proficiency Testing and Control in Kenya. *J Food Prot* 2020; **83**: 142-146 [PMID: 31855611 DOI: 10.4315/0362-028X.JFP-19-292]
- 11 **Cai D**, Yu J, Qiu J, He B, Chen Z, Yan M, Liu Q. Dynamic changes of Sonic Hedgehog signaling pathway in gastric mucosa of rats with MNNG-induced gastric precancerous lesions. *J Cell Physiol* 2019; **234**: 10827-10834 [PMID: 30537251 DOI: 10.1002/jcp.27908]
- 12 **Wu S**, Chen M, Huang J, Zhang F, Lv Z, Jia Y, Cui YZ, Sun LZ, Wang Y, Tang Y, Verhoeft KR, Li Y, Qin Y, Lin X, Guan XY, Lam KO. ORAI2 Promotes Gastric Cancer Tumorigenicity and Metastasis through PI3K/Akt Signaling and MAPK-Dependent Focal Adhesion Disassembly. *Cancer Res* 2021; **81**: 986-1000 [PMID: 33310726 DOI: 10.1158/0008-5472.CAN-20-0049]
- 13 **Li Q**, Ni Y, Zhang L, Jiang R, Xu J, Yang H, Hu Y, Qiu J, Pu L, Tang J, Wang X. HIF-1 α -induced expression of m6A reader YTHDF1 drives hypoxia-induced autophagy and malignancy of hepatocellular carcinoma by promoting ATG2A and ATG14 translation. *Signal Transduct Target Ther* 2021; **6**: 76 [PMID: 33619246 DOI: 10.1038/s41392-020-00453-8]
- 14 **Yang J**, Zhang X, Cao J, Xu P, Chen Z, Wang S, Li B, Zhang L, Xie L, Fang L, Xu Z. Circular RNA UBE2Q2 promotes malignant progression of gastric cancer by regulating signal transducer and activator of transcription 3-mediated autophagy and glycolysis. *Cell Death Dis* 2021; **12**: 910 [PMID: 34611143 DOI: 10.1038/s41419-021-04216-3]
- 15 **Xu J**, Patel NH, Gewirtz DA. Triangular Relationship between p53, Autophagy, and Chemotherapy Resistance. *Int J Mol Sci* 2020; **21** [PMID: 33256191 DOI: 10.3390/ijms21238991]
- 16 **Zachari M**, Ganley IG. The mammalian ULK1 complex and autophagy initiation. *Essays Biochem* 2017; **61**: 585-596 [PMID: 29233870 DOI: 10.1042/EBC20170021]
- 17 **Uno Y**. Prevention of gastric cancer by Helicobacter pylori eradication: A review from Japan. *Cancer Med* 2019; **8**: 3992-4000 [PMID: 31119891 DOI: 10.1002/cam4.2277]
- 18 **Mannion A**, Dzink-Fox J, Shen Z, Piazuelo MB, Wilson KT, Correa P, Peek RM Jr, Camargo MC, Fox JG. Helicobacter pylori Antimicrobial Resistance and Gene Variants in High- and Low-Gastric-Cancer-Risk Populations. *J Clin Microbiol* 2021; **59** [PMID: 33692136 DOI: 10.1128/JCM.03203-20]
- 19 **Nakayama C**, Yamamichi N, Tomida S, Takahashi Y, Kageyama-Yahara N, Sakurai K, Takeuchi C, Inada KI, Shioyama K, Nagae G, Ono S, Tsuji Y, Niimi K, Fujishiro M, Aburatani H, Tsutsumi Y, Koike K. Transduced caudal-type homeobox (CDX) 2/CDX1 can induce growth inhibition on CDX-deficient gastric cancer by rapid intestinal differentiation. *Cancer Sci* 2018; **109**: 3853-3864 [PMID: 30289576 DOI: 10.1111/cas.13821]
- 20 **Sobecki M**, Mrouj K, Colinge J, Gerbe F, Jay P, Krasinska L, Dulic V, Fisher D. Cell-Cycle Regulation Accounts for Variability in Ki-67 Expression Levels. *Cancer Res* 2017; **77**: 2722-2734 [PMID: 28283655 DOI: 10.1158/0008-5472.CAN-16-0707]
- 21 **Fujita Y**, Uesugi N, Sugimoto R, Eizuka M, Toya Y, Akasaka R, Matsumoto T, Sugai T. Analysis of clinicopathological and molecular features of crawling-type gastric adenocarcinoma. *Diagn Pathol* 2020; **15**: 111 [PMID: 32943104 DOI: 10.1186/s13000-020-01026-7]
- 22 **Scavo MP**, Rizzi F, Depalo N, Armentano R, Coletta S, Serino G, Fanizza E, Pesole PL, Cervellera A, Carella N, Curri ML, Giannelli G. Exosome Released FZD10 Increases Ki-67 Expression via Phospho-ERK1/2 in Colorectal and Gastric Cancer. *Front Oncol* 2021; **11**: 730093 [PMID: 34671555 DOI: 10.3389/fonc.2021.730093]

- 23 **Devis-Jauregui L**, Eritja N, Davis ML, Matias-Guiu X, Llobet-Navàs D. Autophagy in the physiological endometrium and cancer. *Autophagy* 2021; **17**: 1077-1095 [PMID: 32401642 DOI: 10.1080/15548627.2020.1752548]
- 24 **Jiao T**, Wu J, Casper DP, Davis DL, Brown MA, Zhao S, Liang J, Lei Z, Holloway B. Feeding Sheep Cobalt and Oregono Essential Oil Alone or in Combination on Ruminant Nutrient Digestibility, Fermentation, and Fiber Digestion Combined With Scanning Electron Microscopy. *Front Vet Sci* 2021; **8**: 639432 [PMID: 34195240 DOI: 10.3389/fvets.2021.639432]
- 25 **Kim HM**, Kim ES, Koo JS. Expression of Autophagy-Related Proteins in Different Types of Thyroid Cancer. *Int J Mol Sci* 2017; **18** [PMID: 28257096 DOI: 10.3390/ijms18030540]
- 26 **Jeong SJ**, Zhang X, Rodriguez-Velez A, Evans TD, Razani B. p62/SQSTM1 and Selective Autophagy in Cardiometabolic Diseases. *Antioxid Redox Signal* 2019; **31**: 458-471 [PMID: 30588824 DOI: 10.1089/ars.2018.7649]
- 27 **Fattahi S**, Amjadi-Moheb F, Tabaripour R, Ashrafi GH, Akhavan-Niaki H. PI3K/AKT/mTOR signaling in gastric cancer: Epigenetics and beyond. *Life Sci* 2020; **262**: 118513 [PMID: 33011222 DOI: 10.1016/j.lfs.2020.118513]
- 28 **Zhou J**, Jiang YY, Chen H, Wu YC, Zhang L. Tanshinone I attenuates the malignant biological properties of ovarian cancer by inducing apoptosis and autophagy via the inactivation of PI3K/AKT/mTOR pathway. *Cell Prolif* 2020; **53**: e12739 [PMID: 31820522 DOI: 10.1111/cpr.12739]
- 29 **Courtney R**, Ngo DC, Malik N, Ververis K, Tortorella SM, Karagiannis TC. Cancer metabolism and the Warburg effect: the role of HIF-1 and PI3K. *Mol Biol Rep* 2015; **42**: 841-851 [PMID: 25689954 DOI: 10.1007/s11033-015-3858-x]
- 30 **Vacek JC**, Behera J, George AK, Kamat PK, Kalani A, Tyagi N. Tetrahydrocurcumin ameliorates homocysteine-mediated mitochondrial remodeling in brain endothelial cells. *J Cell Physiol* 2018; **233**: 3080-3092 [PMID: 28833102 DOI: 10.1002/jcp.26145]
- 31 **Zeng J**, Yan R, Pan H, You F, Cai T, Liu W, Zheng C, Zhao Z, Gong D, Chen L, Zhang Y. Weipixiao attenuate early angiogenesis in rats with gastric precancerous lesions. *BMC Complement Altern Med* 2018; **18**: 250 [PMID: 30200948 DOI: 10.1186/s12906-018-2309-3]
- 32 **Liu W**, Zhao ZM, Liu YL, Pan HF, Lin LZ. Weipiling ameliorates gastric precancerous lesions in Atp4a(-/-) mice. *BMC Complement Altern Med* 2019; **19**: 318 [PMID: 31744486 DOI: 10.1186/s12906-019-2718-y]
- 33 **Chen F**, Chen J, Yang L, Liu J, Zhang X, Zhang Y, Tu Q, Yin D, Lin D, Wong PP, Huang D, Xing Y, Zhao J, Li M, Liu Q, Su F, Su S, Song E. Extracellular vesicle-packaged HIF-1 α -stabilizing lncRNA from tumour-associated macrophages regulates aerobic glycolysis of breast cancer cells. *Nat Cell Biol* 2019; **21**: 498-510 [PMID: 30936474 DOI: 10.1038/s41556-019-0299-0]
- 34 **Yang J**, Ren B, Yang G, Wang H, Chen G, You L, Zhang T, Zhao Y. The enhancement of glycolysis regulates pancreatic cancer metastasis. *Cell Mol Life Sci* 2020; **77**: 305-321 [PMID: 31432232 DOI: 10.1007/s00018-019-03278-z]
- 35 **Brooks GA**. Lactate as a fulcrum of metabolism. *Redox Biol* 2020; **35**: 101454 [PMID: 32113910 DOI: 10.1016/j.redox.2020.101454]
- 36 **Contreras-Baeza Y**, Sandoval PY, Alarcón R, Galaz A, Cortés-Molina F, Alegría K, Baeza-Lehnert F, Arce-Molina R, Guequén A, Flores CA, San Martín A, Barros LF. Monocarboxylate transporter 4 (MCT4) is a high affinity transporter capable of exporting lactate in high-lactate microenvironments. *J Biol Chem* 2019; **294**: 20135-20147 [PMID: 31719150 DOI: 10.1074/jbc.RA119.009093]
- 37 **Dong Z**, Yang J, Li L, Tan L, Shi P, Zhang J, Zhong X, Ge L, Wu Z, Cui H. FOXO3a/SIRT6 axis suppresses aerobic glycolysis in melanoma. *Int J Oncol* 2020; **56**: 728-742 [PMID: 32124950 DOI: 10.3892/ijo.2020.4964]
- 38 **Jia Y**, Li HY, Wang Y, Wang J, Zhu JW, Wei YY, Lou L, Chen X, Mo SJ. Crosstalk between hypoxia-sensing ULK1/2 and YAP-driven glycolysis fuels pancreatic ductal adenocarcinoma development. *Int J Biol Sci* 2021; **17**: 2772-2794 [PMID: 34345207 DOI: 10.7150/ijbs.60018]
- 39 **Liu Y**, Gu W. The complexity of p53-mediated metabolic regulation in tumor suppression. *Semin Cancer Biol* 2022; **85**: 4-32 [PMID: 33785447 DOI: 10.1016/j.semcancer.2021.03.010]
- 40 **Zhu J**, Ao H, Liu M, Cao K, Ma J. UBE2T promotes autophagy via the p53/AMPK/mTOR signaling pathway in lung adenocarcinoma. *J Transl Med* 2021; **19**: 374 [PMID: 34461934 DOI: 10.1186/s12967-021-03056-1]
- 41 **Xu Y**, Tian C, Sun J, Zhang J, Ren K, Fan XY, Wang K, Wang H, Yan YE, Chen C, Shi Q, Dong XP. FBXW7-Induced MTOR Degradation Forces Autophagy to Counteract Persistent Prion Infection. *Mol Neurobiol* 2016; **53**: 706-719 [PMID: 25579381 DOI: 10.1007/s12035-014-9028-7]
- 42 **Chang HW**, Kim MR, Lee HJ, Lee HM, Kim GC, Lee YS, Nam HY, Lee M, Jang HJ, Lee KE, Lee JC, Byun Y, Kim SW, Kim SY. p53/BNIP3-dependent mitophagy limits glycolytic shift in radioresistant cancer. *Oncogene* 2019; **38**: 3729-3742 [PMID: 30664690 DOI: 10.1038/s41388-019-0697-6]
- 43 **Seillier M**, Peugot S, Gayet O, Gauthier C, N'Guessan P, Monte M, Carrier A, Iovanna JL, Dusetti NJ. TP53INP1, a tumor suppressor, interacts with LC3 and ATG8-family proteins through the LC3-interacting region (LIR) and promotes autophagy-dependent cell death. *Cell Death Differ* 2012; **19**: 1525-1535 [PMID: 22421968 DOI: 10.1038/cdd.2012.30]
- 44 **Han JA**, Kim JI, Ongusaha PP, Hwang DH, Ballou LR, Mahale A, Aaronson SA, Lee SW. P53-mediated induction of Cox-2 counteracts p53- or genotoxic stress-induced apoptosis. *EMBO J* 2002; **21**: 5635-5644 [PMID: 12411481 DOI: 10.1093/emboj/cdf591]
- 45 **Mimouna S**, Bazin M, Mograbi B, Darfeuille-Michaud A, Brest P, Hofman P, Vouret-Craviari V. HIF1A regulates xenophagic degradation of adherent and invasive Escherichia coli (AIEC). *Autophagy* 2014; **10**: 2333-2345 [PMID: 25484075 DOI: 10.4161/15548627.2014.984275]
- 46 **Yu CH**, Chu SC, Yang SF, Hsieh YS, Lee CY, Chen PN. Induction of apoptotic but not autophagic cell death by Cinnamomum cassia extracts on human oral cancer cells. *J Cell Physiol* 2019; **234**: 5289-5303 [PMID: 30317581 DOI: 10.1002/jcp.27338]
- 47 **Chen J**, Zhao D, Zhu M, Zhang M, Hou X, Ding W, Sun S, Bu W, Feng L, Ma S, Jia X. Paeoniflorin ameliorates AGEs-induced mesangial cell injury through inhibiting RAGE/mTOR/autophagy pathway. *Biomed Pharmacother* 2017; **89**: 1362-1369 [PMID: 28320103 DOI: 10.1016/j.biopha.2017.03.016]
- 48 **Nazim UM**, Park SY. Attenuation of autophagy flux by 6-shogaol sensitizes human liver cancer cells to TRAIL-induced apoptosis via p53 and ROS. *Int J Mol Med* 2019; **43**: 701-708 [PMID: 30483736 DOI: 10.3892/ijmm.2018.3994]
- 49 **Wu J**, Zhang X, Wang Y, Sun Q, Chen M, Liu S, Zou X. Licochalcone A suppresses hexokinase 2-mediated tumor

glycolysis in gastric cancer *via* downregulation of the Akt signaling pathway. *Oncol Rep* 2018; **39**: 1181-1190 [PMID: 29286170 DOI: 10.3892/or.2017.6155]



Published by **Baishideng Publishing Group Inc**
7041 Koll Center Parkway, Suite 160, Pleasanton, CA 94566, USA
Telephone: +1-925-3991568
E-mail: bpgoffice@wjgnet.com
Help Desk: <https://www.f6publishing.com/helpdesk>
<https://www.wjgnet.com>

